Elliptic master integrals and the one-loop wavefunction of the universe

Amara McCune*
Anthropic STEM Fellow

Matthew D. Schwartz*
Department of Physics, Harvard University

Abstract

The one-loop triangle wavefunction coefficient of a conformally coupled scalar contains master integrals that obey an elliptic differential equation, which suggested that cosmological wavefunction coefficients leave the space of polylogarithms already at one loop. We compute this coefficient in flat space, the seed for de Sitter and power-law backgrounds, and find that it is polylogarithmic. For all site energies it is a combination of dilogarithms, which we give in closed form. The elliptic periods cancel because the residue of the integrand at the poles that carry the curve is a flat-space amplitude, which is rational in the loop momentum. We fix the function space from exact differential equations and the few remaining rational constants numerically. The one-loop box is not polylogarithmic, even with a single external leg at each site. Its soft discontinuity is an elliptic function, which we also give in closed form, and the periods of a K3 surface enter as well. The triangle is therefore the last polygon of this theory that is polylogarithmic.

1 Introduction

Inflation predicts the correlation functions of the primordial density perturbations, and surveys of the microwave background and of the distribution of galaxies measure them. The measurements improve with every survey, while the calculations lag behind. Beyond the simplest models and the lowest orders of perturbation theory, the integrals behind the predictions have resisted computation, and at loop level even the kind of function that the answer should be is mostly unknown.

For scattering amplitudes this last question has been remarkably productive. Feynman integrals evaluate to restricted classes of functions, beginning with polylogarithms and continuing with integrals over elliptic curves and higher-dimensional varieties. Once the class is known, an amplitude can often be constructed from its singularities and symmetries without evaluating any integral. The wavefunction of the universe plays the role in cosmology that amplitudes play at colliders. Its coefficients, one for each graph of perturbation theory, encode the correlations of the fields at the end of inflation, and equal-time correlators follow from them. Over the past decade the computation of these coefficients has absorbed much of the amplitudes toolkit, including canonical differential equations, integration-by-parts reduction and twisted cohomology. The cosmological bootstrap [1, 2] aims to construct correlators from their singularities in the same spirit. It requires the same input, which is the space of functions in which the answer lives.

At tree level the answer is well understood for conformally coupled scalars in de Sitter space and in power-law cosmologies. The flat-space integrand is the canonical form of a cosmological polytope [3], a rational function with simple poles where the energy entering a subgraph vanishes. The

*Work done with Anthropic, but results and views are not endorsed by Anthropic.

wavefunction coefficients are polylogarithms, or their generalizations with non-integer exponents, and they satisfy differential equations of a universal combinatorial form [4–8]. At one loop much less is known. The one-loop graph with two vertices, or sites in the language of this literature, is polylogarithmic [9–11]. Ref. [9] derived differential equations for the one-loop triangle and found that a sector of its master integrals obeys an irreducible second-order equation whose solutions are elliptic integrals. The authors concluded that the triangle wavefunction coefficient involves elliptic functions, and that this "is likely to extend to all polygon graphs with a higher number of sites". They noted that an explicit computation was needed to classify the functions that arise. This would place cosmological loops in contrast with flat-space amplitudes, where elliptic integrals first appear at two loops [12–14].

There were already hints that the situation is more subtle. The one-loop four-point correlator of a conformally coupled scalar with a quartic interaction in de Sitter space, computed in position space, closes in single-valued polylogarithms, because an elliptic sector that is present in anti-de Sitter space cancels [15]. The flat-space in-in triangle is a combination of dilogarithms, while the integrals that are particular to the wavefunction were expected to be more complicated [16]. The one-loop triangle correlator of conformally coupled scalars in de Sitter space has been evaluated in dilogarithms [17]. In each case an observable turned out to be simpler than the integrals that one meets on the way to it.

In this paper we carry out the explicit computation for the triangle and examine the conclusion of ref. [9]. We find that it holds for the master integrals and fails for the wavefunction coefficient. The coefficient is a polylogarithmic function of weight two. With one external leg at each site it is the combination of three dilogarithms in eq. (26). With several legs per site, which is the case needed for expanding backgrounds, it is given by eq. (29). The arguments of its dilogarithms contain ten square roots, all of which become rational with one leg per site. We obtain these results in two steps. On two lines in kinematic space we derive exact differential operators for the loop-integrated coefficient. They factor completely into first-order operators, which fixes the function space. We then determine the few remaining rational constants numerically, and the results agree with the integral to more than 40 digits (section 4).

The reason for the cancellation is visible at the level of residues. We derive the elliptic curve of the triangle from the loop measure and give its periods (section 3). The curve is attached to three poles of the integrand. At these poles the residue of the physical integrand is a flat-space amplitude, which is rational in the loop momentum, so no elliptic curve appears in any residue of the physical integrand (proposition 1). The geometry of the master integrals therefore overestimates the function space of the physical quantity. An integration-by-parts reduction separates the integrand into pieces that are individually more singular than their sum, and the geometry of the pieces need not survive.

The three poles come from the term of the propagator that enforces the boundary condition of the wavefunction at late times. They are known to be absent from equal-time correlators [18, 19], and ref. [9] asked whether correlators then still require elliptic functions. In section 5 we examine the singular lines of the integrands of polygons up to the pentagon, in the dimension where the loop measure is a square root. In every case the correlator integrand has no residue on a line where the loop measure defines an elliptic curve.

The mechanism is special to the triangle. For the one-loop box the residue at the pole of a single site involves two square roots, and the box is not polylogarithmic, even with one leg per site. We give its soft discontinuity in closed form in terms of elliptic integrals. The periods of a K3 surface enter as well, and on one line in kinematic space we determine the box from an exact differential system (section 6). The triangle is therefore the last polygon of this theory that is polylogarithmic.

Section 2 defines the integrand, the loop measure and the kinematics, and section 7 comments on de Sitter space and on open questions. Our methods combine exact reduction with a practice that is standard for multiloop amplitudes [20]. One evaluates an integral to high precision, fits an ansatz in the function space suggested by its cuts, and judges the result on digits that were not used in the fit. Appendix A describes these methods and their relation to other bootstrap methods in cosmology.

2 Setup

In this section we fix the object that the rest of the paper studies. We first recall how the wavefunction coefficients of a conformally coupled scalar in an expanding background are built from flat-space ones. We then write the flat-space integrand of the one-loop triangle, describe the loop measure, and specify the external kinematics. A reader who knows the cosmological polytope literature [3] can skip to section 2.3.

2.1 Wavefunction coefficients and correlators

The late-time state of the fields is described by the wavefunction $\Psi[\phi]$. It is the amplitude for the field to have the spatial profile $\phi(\vec{k})$ at conformal time $\eta_0 \to 0$, given the Bunch–Davies vacuum in the far past. Its logarithm is expanded in powers of the boundary profile,

$$\log \Psi[\phi] \;=\; -\sum_n \frac{1}{n!} \int \prod_{i=1}^{n} \frac{\mathrm{d}^3 k_i}{(2\pi)^3}\; \psi_n(\vec{k}_1, \ldots, \vec{k}_n)\, \phi_{\vec{k}_1} \cdots \phi_{\vec{k}_n}\, (2\pi)^3 \delta^3\Big(\textstyle\sum_i \vec{k}_i\Big)\,, \tag{1}$$

and the functions ψ_n are the wavefunction coefficients. Equal-time correlators follow from the Born rule,

$$\langle \phi_{\vec{k}_1} \cdots \phi_{\vec{k}_n} \rangle \;=\; \frac{\int \mathcal{D}\phi\, |\Psi[\phi]|^2\, \phi_{\vec{k}_1} \cdots \phi_{\vec{k}_n}}{\int \mathcal{D}\phi\, |\Psi[\phi]|^2}\,. \tag{2}$$

The two objects carry the same information, but they are different functions of the momenta. This distinction matters throughout the paper. Sections 2–4 concern a wavefunction coefficient, and section 5 shows that the corresponding correlator has a simpler singularity structure.

We consider a conformally coupled scalar with polynomial self-interactions in a spatially flat FRW background. After the field is rescaled by the scale factor, its free action is that of a massless field in flat space. The expansion survives only as a power of conformal time, $(-\eta)^{-(1+\sigma)}$, multiplying each interaction vertex. For a cubic interaction in de Sitter space $\sigma = 0$. In flat space the factor is absent, so the flat-space coefficient is the integrand of the site integrals below and not a special value of σ. We work on the rotated contour $\eta = it$ with $t > 0$. On this contour a leg of energy X in the Bunch–Davies state contributes e^{-Xt}, and the vertex factor is $t^{-(1+\sigma)}$ up to a phase. Because

$$t^{-(1+\sigma)} \;=\; \frac{1}{\Gamma(1+\sigma)} \int_0^\infty \mathrm{d}\omega\; \omega^\sigma\, e^{-\omega t}\,, \tag{3}$$

each vertex factor can be traded for a shift of the energy flowing into that vertex [3, 7]. A coefficient in the expanding background is therefore an integral of the flat-space coefficient over shifted energies,

$$\psi_n^{(\sigma)}(X; y) \;\propto\; \int_0^\infty \prod_v \mathrm{d}\omega_v\, \omega_v^\sigma\; \psi_n(X + \omega; y)\,, \tag{4}$$

where ψ_n without a superscript denotes the flat-space coefficient. Here X_v is the total energy of the external legs at site v, and y_e is the energy of the internal edge e. We call the integrals in eq. (4) the site integrals. The flat-space coefficient is thus the seed for every background of this type, and sections 3 and 4 study it directly. We comment on the site integrals for de Sitter space in section 7.

2.2 The flat-space integrand

The flat-space coefficients are computed from integrals over the rotated times $t_v > 0$. Each site contributes $e^{-X_v t_v}$, and each internal edge contributes the propagator that vanishes at the late-time boundary,

$$G_y(t,t') \;=\; \frac{1}{2y}\Big[e^{-y|t-t'|} - e^{-y(t+t')}\Big]\,. \tag{5}$$

We strip the coupling constants and an overall phase, so that every ψ_n below is a positive rational function of the energies. The first term in eq. (5) is the time-ordered propagator of flat space. The second term is fixed by the boundary condition at $t = 0$, and it factorizes into a product of two functions of a single time. This second term has no counterpart in a scattering amplitude, and it is the origin of the elliptic curve of section 3.

The simplest examples show the pattern. One site with no edges gives $\psi_1 = 1/X$, and two sites joined by an edge give

$$\psi_2 \;=\; \int_0^\infty \mathrm{d}t_1\,\mathrm{d}t_2\; e^{-X_1t_1-X_2t_2}\,G_y(t_1,t_2) \;=\; \frac{1}{(X_1+X_2)(X_1+y)(X_2+y)}\,. \tag{6}$$

Each denominator is the total energy flowing into a connected set of sites, which is the sum of the X_v in the set and of the y_e of the edges that leave it. We call this the energy of the subgraph induced on the set. This rule holds for every tree graph [3]. Energy is not conserved because time translations are broken by the boundary, and the coefficient is singular where the energy entering a subgraph vanishes. At one loop this rule accounts for some of the denominators but not all of them.

We now turn to the one-loop triangle, the graph with three sites and three edges shown in figure 1. Its sites carry energies X_1, X_2, X_3, and its edges carry energies y_{12}, y_{23}, y_{31}, where y_{vw} joins sites v and w. The time integrals give

$$\psi_3(X;y) \;=\; \frac{2\,\mathcal{N}(X;y)}{q_{\mathcal{G}}\,\prod_{i=1}^{9} q_i(X;y)}\,, \qquad q_{\mathcal{G}} = X_1+X_2+X_3\,, \tag{7}$$

with ten linear factors in the denominator. Besides the total energy $q_{\mathcal{G}}$ they are

$$\begin{aligned}
&X_1+y_{12}+y_{31}\,, \quad X_2+y_{12}+y_{23}\,, \quad X_3+y_{23}+y_{31}\,,\\
&X_1+X_2+y_{23}+y_{31}\,, \quad X_2+X_3+y_{12}+y_{31}\,, \quad X_1+X_3+y_{12}+y_{23}\,,\\
&q_{\mathcal{G}}+2y_{12}\,, \quad q_{\mathcal{G}}+2y_{23}\,, \quad q_{\mathcal{G}}+2y_{31}\,.
\end{aligned} \tag{8}$$

The numerator $\mathcal{N}$ is an irreducible homogeneous quartic polynomial with positive coefficients, which we give in the ancillary files. It is generated by a recursion that cuts one edge at a time and expresses ψ_3 through tree coefficients of the three-site chain [3].

The total energy and the first two rows of eq. (8) follow the subgraph rule stated above, for the whole graph, for a single site, and for a pair of sites. The factors in the last row do not. The factor $q_{\mathcal{G}} + 2y_e$ counts the edge e twice, and it is the total energy of the chain obtained by cutting e open, with both ends of e treated as external legs. It arises from the second term of the propagator (5). The three factors $q_{\mathcal{G}} + 2y_e$ play a special role in this paper. Every elliptic curve that we find in the triangle involves one of them, and they are absent from the correlator integrand, as we show in section 5.

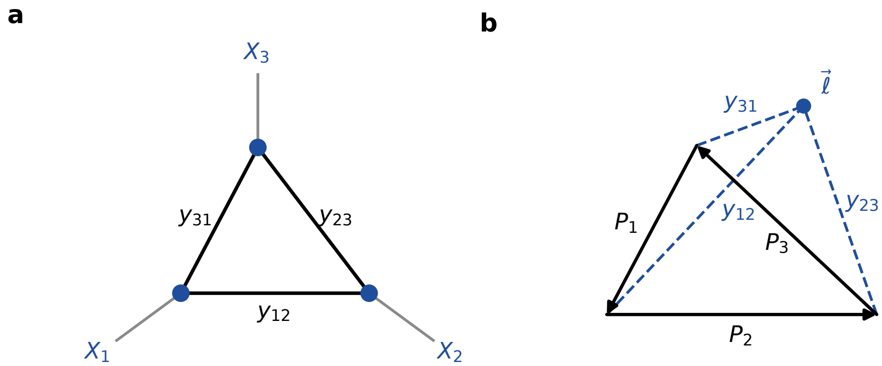

Figure 1: (a) The one-loop graph with three sites. Each site carries the energy X_v of its external legs, and each edge the energy y_e of the internal line. (b) The loop measure. The external momenta form a triangle with sides P_v, and the edge energies are the distances from the loop momentum $\vec{\ell}$ to its corners. In general $\vec{\ell}$ does not lie in the plane of the triangle.

2.3 The loop measure

The edge energies depend on the loop momentum $\vec{\ell}$ through $y_{12} = |\vec{\ell}|$, $y_{23} = |\vec{\ell} + \vec{P}_2|$ and $y_{31} = |\vec{\ell} - \vec{P}_1|$, where $\vec{P}_v$ is the total momentum entering site v and $\vec{P}_1 + \vec{P}_2 + \vec{P}_3 = 0$. The integrand depends on $\vec{\ell}$ only through these three lengths, so we use them as integration variables. Intuitively, the three edge energies are the distances from the point $\vec{\ell}$ to the corners of the triangle formed by the external momenta (figure 1). In three dimensions three distances fix a point up to reflection through the plane of the triangle. The Jacobian is the product of the three distances divided by six times the volume of the tetrahedron with apex $\vec{\ell}$. The reflection doubles it, which gives

$$\mathrm{d}^3\ell \;=\; 4\sqrt{2}\, B(y;P)^{-1/2}\, y_{12}\, y_{23}\, y_{31}\, \mathrm{d}y_{12}\, \mathrm{d}y_{23}\, \mathrm{d}y_{31}\,, \tag{9}$$

where B is the Cayley–Menger determinant of that tetrahedron,

$$B(y;P) \;=\; \det \begin{pmatrix} 0 & 1 & 1 & 1 & 1 \\ 1 & 0 & P_2^2 & P_1^2 & y_{12}^2 \\ 1 & P_2^2 & 0 & P_3^2 & y_{23}^2 \\ 1 & P_1^2 & P_3^2 & 0 & y_{31}^2 \\ 1 & y_{12}^2 & y_{23}^2 & y_{31}^2 & 0 \end{pmatrix}, \tag{10}$$

and $P_v = |\vec{P}_v|$. The integration region is $B > 0$, where the tetrahedron exists. The polynomial B is quadratic in each y_e^2. This change of variables is the Baikov representation of the Feynman-integral literature, and it is the form in which ref. [9] studied the triangle.

The object of this paper is the loop-integrated coefficient, which we normalize as

$$V(X;P) \;=\; \int_{B>0} B(y;P)^{-1/2+\varepsilon}\, y_{12}\, y_{23}\, y_{31}\, q_{\mathcal{G}}\, \psi_3(X;y)\, \mathrm{d}^3y \;\xrightarrow{\varepsilon\to 0}\; \frac{q_{\mathcal{G}}}{4\sqrt{2}} \int \mathrm{d}^3\ell\, \psi_3\,. \tag{11}$$

The integrand falls as $|\vec{\ell}|^{-5}$ at large loop momentum, so V is finite in three dimensions. The exponent ε continues the measure to $d = 3 + 2\varepsilon$ dimensions. We need it because the individual master integrals of section 3 have poles at $\varepsilon = 0$, which cancel in V. The square root $B^{-1/2}$ is what distinguishes this integral from the integrals over rational functions that appear at tree level, and it is the second ingredient of the elliptic curve.

2.4 Kinematics

The coefficient V depends on the site energies X_v and on the momentum magnitudes P_v, which must satisfy the triangle inequalities. If a single external leg is attached to each site, its energy equals the magnitude of its momentum, so that

$$X_v \;=\; P_v\,, \qquad v = 1, 2, 3\,. \tag{12}$$

With several legs at a site, X_v exceeds P_v unless the legs are collinear. We refer to eq. (12) as the case of one leg per site. Ref. [9] studies the differential equations along lines of the form $X = (\alpha\lambda, \lambda, 1)$. We take $\alpha = 2$ and study the line

$$X \;=\; P \;=\; (2\lambda,\, \lambda,\, 1)\,, \qquad \tfrac{1}{3} < \lambda < 1\,, \tag{13}$$

where the range of λ is set by the triangle inequalities. The differential equations of sections 3 and 4 are obtained on this line. The restriction to one leg per site is significant. The site integrals of eq. (4) shift X_v at fixed P_v, so every coefficient in an expanding background samples V away from eq. (12). We treat general site energies in section 4.5.

3 The elliptic sector

In this section we describe the elliptic curve that appears in the triangle and the integrals that carry it. We first organize V into a finite set of basis integrals. We then exhibit the curve, give its periods and the differential operator that they satisfy, and summarize what can be computed explicitly. The section establishes that individual pieces of V are elliptic. Whether V itself is elliptic is a separate question, which we answer in section 4.

3.1 Master integrals

The integrand of eq. (11) is a polynomial divided by a product of linear factors, multiplied by a power of B. We call it the physical integrand, to distinguish it from the integrands of the master integrals introduced below. All such integrals belong to the family

$$I[\mathcal{Q}; n] \;=\; \int_{B>0} B(y; P)^{-1/2+\varepsilon}\, \frac{\mathcal{Q}(y)}{\prod_{i=1}^{9} q_i(X; y)^{n_i}}\, \mathrm{d}^3 y\,, \tag{14}$$

where $\mathcal{Q}$ is a polynomial, the q_i are the nine factors of eq. (8), and the n_i are non-negative integers. Integration-by-parts identities relate the members of this family linearly, with coefficients that are rational functions of the kinematics and of ε. As for Feynman integrals, the family is spanned by a finite number of basis elements, which are called master integrals. We group them into sectors according to which of the factors q_i appear in the denominator. The derivative of a master integral with respect to λ is again a combination of master integrals from its own sector and from sectors with fewer denominators. Each sector therefore has its own homogeneous differential equation, and this equation decides which functions the sector can produce.

The sectors built only from the first six factors of eq. (8) produce polylogarithms on the line (13). The three factors $q_{\mathcal{G}} + 2y_e$ behave differently. Ref. [9] found that the sector with the single denominator $q_{\mathcal{G}} + 2y_{12}$ contains a block of master integrals whose homogeneous equation is of second order and cannot be factored. The same holds for $q_{\mathcal{G}} + 2y_{23}$ and $q_{\mathcal{G}} + 2y_{31}$ after a permutation of the sites. We call these three sectors the elliptic sectors.

3.2 The curve

The curve can be read off from the loop measure. The essential point is that the integrals of this sector are not functions of the squares y_e^2 alone, although B is. In the sector with denominator $q_{\mathcal{G}} + 2y_{12}$ we take the residue at $y_{12} = -q_{\mathcal{G}}/2$, which leaves an integral over y_{23} and y_{31}. The denominator no longer depends on these variables, so the only structure left is the square root of B. In terms of $z_e = y_e^2$ the polynomial B is quadratic. Along the ray $z_{31} = s\, z_{23}$ its leading behaviour at large z_{23} is

$$B \;=\; -A(s)\, z_{23}^2 + O(z_{23})\,, \qquad A(s) \;=\; 2\big[P_2^2\, s^2 - \big(P_1^2 + P_2^2 - P_3^2\big)\, s + P_1^2\big]\,, \tag{15}$$

and $A(s)$ does not depend on y_{12}. If the rest of the integrand were a rational function of s, the square root of the quadratic $A(s)$ would define a curve of genus zero. A master integral with unit numerator has the measure $\mathrm{d}y_{23}\,\mathrm{d}y_{31}$ and not $\mathrm{d}z_{23}\,\mathrm{d}z_{31}$, however. Its integrand at large y_{23} and y_{31} is proportional to $\mathrm{d}s/\sqrt{s\,A(s)} = 2\,\mathrm{d}\tau/\sqrt{A(\tau^2)}$ with $\tau = y_{31}/y_{23}$. The square root of the quartic $A(\tau^2)$ defines the elliptic curve

$$w^2 \;=\; P_2^2\, \tau^4 - \big(P_1^2 + P_2^2 - P_3^2\big)\, \tau^2 + P_1^2\,. \tag{16}$$

The discriminant of $A(s)$ is proportional to the Källén function of the P_v^2, so the four branch points are distinct whenever the momenta form a non-degenerate triangle. Two features of eq. (16) will matter below. The curve depends on the momenta P_v only, and not on the site energies X_v. It is also located at infinity on the surface $q_{\mathcal{G}} + 2y_{12} = 0$, where y_{23} and y_{31} become large at fixed y_{12}. This is not a region of real loop momentum. An integrand can be sensitive to the curve only through its behaviour at large y_{23} and y_{31} on that surface. On the line (13) the curve is isomorphic to the Legendre curve with modulus

$$m(\lambda) \;=\; \frac{\lambda^2 - 1}{9\lambda^2 - 1}\,, \tag{17}$$

which is the modulus identified in ref. [9]. The sectors with denominators $q_{\mathcal{G}} + 2y_{23}$ and $q_{\mathcal{G}} + 2y_{31}$ have curves of the same form with the momenta permuted. The three curves are not isomorphic to one another.

3.3 Periods and their differential equation

On the line (13) the irreducible second-order operator of the elliptic sector is [9]

$$\mathcal{L}_2 \;=\; \frac{\mathrm{d}^2}{\mathrm{d}\lambda^2} + \frac{45\lambda^4 - 30\lambda^2 + 1}{\lambda\,(\lambda^2-1)(9\lambda^2-1)}\,\frac{\mathrm{d}}{\mathrm{d}\lambda} + \frac{27\lambda^2 - 10}{(\lambda^2-1)(9\lambda^2-1)}\,. \tag{18}$$

Its solutions are complete elliptic integrals of the first kind with an algebraic prefactor. They are $K(m)/\sqrt{1-9\lambda^2}$ and $K(1-m)/\sqrt{1-9\lambda^2}$ with $m = m(\lambda)$, where $K(m) = \int_0^{\pi/2} (1 - m\sin^2\theta)^{-1/2}\,\mathrm{d}\theta$. On the physical interval $\frac{1}{3} < \lambda < 1$ a basis of real solutions is

$$\varpi_0(\lambda) \;=\; \frac{1}{\lambda}\, K\Big(\frac{1-\lambda^2}{8\lambda^2}\Big)\,, \qquad \varpi_1(\lambda) \;=\; \frac{1}{\lambda}\, K\Big(\frac{9\lambda^2-1}{8\lambda^2}\Big)\,. \tag{19}$$

The first is analytic at $\lambda = 1$ and has a logarithmic singularity at $\lambda = \frac{1}{3}$, and the second has the opposite behaviour. The operator $\mathcal{L}_2$ has regular singular points at $\lambda = 0, \pm\frac{1}{3}, \pm 1$ and ∞. At each finite singular point the two local exponents coincide, so that one solution is analytic there and the other has a logarithm. Both ends of the physical interval $\frac{1}{3} < \lambda < 1$ are singular points of this kind. We use this fact in section 4, because a function that contains the periods (19) inherits their logarithmic singularities.

The operator $\mathcal{L}_2$ does not depend on whether the denominator is $q_{\mathcal{G}} + 2y_{12}$ or $q_{\mathcal{G}} + y_{12}$, because the curve (16) does not depend on the position of the pole in y_{12}. The triangle section of ref. [9] prints the latter, while its two-site section and the time integrals of section 2.2 give the former, which we use throughout. The choice affects the master integrals below the elliptic block and the assembled coefficient, but not the curve.

3.4 What can be computed in the elliptic sector

With the periods in hand, the master integrals of the elliptic sector can be computed by the methods developed for elliptic Feynman integrals [21–23]. The sector with denominator $q_{\mathcal{G}} + 2y_{12}$ has nine master integrals on the line (13), which couple to seven master integrals without any linear denominator. A change of basis brings the differential equation into a form whose connection is a polynomial of degree three in ε. The change of basis is built from ϖ_0, its derivative, the square root of a quartic polynomial in λ, and a small number of further transcendental functions. The part of the connection of order ε^0 is nilpotent, and it couples the elliptic block to the master integrals without linear denominators. The solution is therefore a finite sum of iterated integrals at each order in ε, whose integration kernels are built from rational functions of λ, the periods (19) and algebraic functions. The quartic is the curve (16) evaluated at a marked point, so a single elliptic curve is involved. The constants that arise when the iterated integrals are taken from one point of the line to another have closed forms in terms of incomplete elliptic integrals, logarithms and algebraic numbers. The poles of the master integrals at $\varepsilon = 0$ are obtained in closed form. We have verified these statements independently, and the record is part of the ancillary files.

The master integrals of these sectors are therefore elliptic. As a check of the method, we derived the differential operator of a master integral of the sector with the reduction of section 4, and it has an irreducible second-order factor equivalent to $\mathcal{L}_2$. It is therefore natural to expect, as ref. [9] concluded, that the triangle coefficient is an elliptic function of the kinematics. In the next section we show that this expectation is not borne out.

4 The loop-integrated coefficient

In this section we ask whether the elliptic periods of section 3 appear in the coefficient V itself. They do not. We first show that the residue of the physical integrand on the factors $q_{\mathcal{G}} + 2y_e$ is a flat-space amplitude. As a consequence, no residue of the integrand involves an elliptic curve (proposition 1). This is the mechanism to which we trace the cancellation. We then derive a differential equation that V satisfies on the line (13), and show that it factors completely into first-order operators. In section 4.4 we solve the equation and obtain V in closed form with one leg per site. In section 4.5 we extend the result to general site energies.

4.1 Why the periods cancel

A master integral of the elliptic sector has a pole at $q_{\mathcal{G}} + 2y_{12} = 0$, and its residue there contains the holomorphic differential $\mathrm{d}\tau/w$ of the curve (16). The coefficient V is a particular combination of master integrals, and the question is what the combination does at this pole. The residue of the integrand (7) is

$$\operatorname*{Res}_{y_{12}=-q_{\mathcal{G}}/2} \psi_3 \;=\; \frac{1}{2\, q_{\mathcal{G}} \left(y_{23}^2 - E_2^2\right)\left(y_{31}^2 - E_1^2\right)}\,, \qquad E_1 = \tfrac{1}{2}(X_2 + X_3 - X_1)\,, \quad E_2 = \tfrac{1}{2}(X_1 + X_3 - X_2)\,. \tag{20}$$

This has a simple interpretation. The factor $q_{\mathcal{G}} + 2y_{12}$ is the total energy of the chain obtained by cutting the edge y_{12}, and the residue of a tree-level coefficient at its total-energy pole is the flat-space amplitude [3]. Equation (20) is a product of two Feynman propagators, in which E_1 and E_2 are the energies that flow through the remaining edges. It therefore depends on the edge energies y_{23} and y_{31} only through their squares, that is, through the loop momentum and not through its magnitude. This is the origin of the cancellation. To state it precisely, we write

$$\omega \;=\; q_{\mathcal{G}}\, \psi_3\, y_{12}\, y_{23}\, y_{31}\, \mathrm{d}y_{12}\, \mathrm{d}y_{23}\, \mathrm{d}y_{31} \tag{21}$$

for the rational part of the integrand of eq. (11), which has poles on the nine planes (8).

Proposition 1. *Let the X_v be arbitrary and the P_v generic.*

1. *The residue of ω on the plane $q_{\mathcal{G}} + 2y_{12} = 0$ is*

$$-\frac{q_{\mathcal{G}}}{16}\, \frac{\mathrm{d}z_{23}\, \mathrm{d}z_{31}}{\left(z_{23} - E_2^2\right)\left(z_{31} - E_1^2\right)}\,, \qquad z_e = y_e^2\,, \tag{22}$$

   and the polynomial B on this plane is of total degree two in z_{23} and z_{31}. The same holds on the other two planes $q_{\mathcal{G}} + 2y_e = 0$.

2. *The nine planes meet in pairs along 36 lines. Three of the lines lie at infinity. On 12 lines B is a quadratic polynomial in the coordinate along the line. On the remaining 21 lines B is a quartic polynomial with distinct roots, so that $w^2 = B$ is an elliptic curve. Each of these 21 lines lies in one of the planes $q_{\mathcal{G}} + 2y_e = 0$.*

3. *On 9 of the 21 lines the residue of ω vanishes. On each of the other 12 a single edge energy y varies along the line, and $B = b(y^2)$ with b a quadratic polynomial. The residue of $\omega/\sqrt{B}$ is*

$$\pm\frac{q_{\mathcal{G}}}{16}\, \frac{\mathrm{d}Z}{\left(Z - E^2\right)\sqrt{b(Z)}}\,, \qquad Z = y^2\,, \tag{23}$$

   with E one of the energies E_i of the corresponding plane. The same is true if $B^{-1/2}$ is replaced by $B^{-1/2+\varepsilon}$.

The form (23) lives on the curve $w^2 = b(Z)$, which has genus zero. The physical integrand therefore has no residue, on any plane or line, that involves one of the 21 elliptic curves. A master integral with a constant numerator and the same two denominators has the residue $\mathrm{d}y/\sqrt{b(y^2)}$, which is the holomorphic differential of the elliptic curve.

The proof is short. Part 1 is eq. (20) multiplied by the measure, with $y_{23}\, y_{31}\, \mathrm{d}y_{23}\, \mathrm{d}y_{31} = \frac{1}{4}\, \mathrm{d}z_{23}\, \mathrm{d}z_{31}$, and the statement about B follows from eq. (10). Part 2 is a direct computation. The 12 lines with a quadratic B are those on which two subgraph energies vanish, and all three edge energies vary along them. Part 3 follows from part 1. The form (22) has poles only at $y_{23} = \pm E_2$ and $y_{31} = \pm E_1$. On the plane $q_{\mathcal{G}} + 2y_{12} = 0$ these are the lines where the energy of site 1, of site 2, or of the pairs of sites $\{2, 3\}$ or $\{1, 3\}$ vanishes. This gives four lines for each of the three planes. The other planes cross $q_{\mathcal{G}} + 2y_{12} = 0$ along lines where the form (22) is regular. Parts 2 and 3 are also confirmed by computer algebra.

The master integrals do not share this property. If the residue (20) is decomposed into partial fractions in y_{23} and y_{31}, each of the four terms $1/[(y_{23} \mp E_2)(y_{31} \mp E_1)]$ has a non-zero coefficient of the holomorphic differential $\mathrm{d}\tau/w$ of the curve (16). The four coefficients are equal in magnitude, with signs $(+,-,-,+)$, and their sum vanishes. The elliptic periods therefore appear in the pieces into which an integration-by-parts reduction naturally separates V, and cancel between them.

Proposition 1 holds for all values of X_v and P_v. It therefore applies with several legs per site, where the master integrals have many more elliptic sectors (section 4.5). It does not by itself determine the function class of V, because the integral over the region $B > 0$ is not a sum of residues. It shows that the elliptic curves of the master integrals are invisible to every residue of the physical integrand. For the function class we turn to the differential equation.

4.2 The differential equation

We reduce the integrand of eq. (11) to master integrals with the integration-by-parts identities of the family (14), as described in appendix A. The result expresses V and its λ-derivatives through the same master integrals. Eliminating the master integrals gives a linear differential operator that annihilates V. At generic ε it has order 20. Its limit as $\varepsilon \to 0$,

$$\mathcal{L}_0 \;=\; \sum_{i=0}^{20} c_i(\lambda)\,\frac{\mathrm{d}^i}{\mathrm{d}\lambda^i}\,, \qquad \mathcal{L}_0\, V \;=\; 0\,, \tag{24}$$

has polynomial coefficients c_i of degree 132 to 152, and we give it in the ancillary files. Its singular points are $\lambda = 0, \pm\frac{1}{3}, \pm 1$ and ∞, which are the singular points of $\mathcal{L}_2$, together with apparent singularities at which all solutions are analytic.

The limit must be taken after the reduction. If one sets $\varepsilon = 0$ from the start, the reduction acquires additional relations and produces an operator of order 14 that does not annihilate V. We attribute this to the poles of the individual master integrals at $\varepsilon = 0$, through which terms of order ε in the reduction contribute to the finite part. The order-14 operator is a right factor of $\mathcal{L}_0$. The operator $\mathcal{L}_0$ annihilates the numerical values of V on the line to their accuracy, and the operator of order 14 does not (appendix A).

4.3 Complete factorization

The operator $\mathcal{L}_0$ factors completely over the rational functions of λ,

$$\mathcal{L}_0 \;=\; c_{20}(\lambda)\left(\frac{\mathrm{d}}{\mathrm{d}\lambda} - \frac{r_{20}'}{r_{20}}\right)\left(\frac{\mathrm{d}}{\mathrm{d}\lambda} - \frac{r_{19}'}{r_{19}}\right)\cdots\left(\frac{\mathrm{d}}{\mathrm{d}\lambda} - \frac{r_{1}'}{r_{1}}\right), \tag{25}$$

where every r_k is a rational function of λ and a prime denotes $\mathrm{d}/\mathrm{d}\lambda$. The factorization is exact. We obtained it by right division in the ring of differential operators with coefficients in $\mathbb{Q}(\lambda)$.

A solution of a product of first-order operators is obtained by solving the factors one at a time, and each step is an integration against a rational function. Equation (25) therefore shows that $V(\lambda)$ is an iterated integral of rational one-forms, that is, a function of polylogarithmic type. An elliptic period would require an irreducible factor of second order, as $\mathcal{L}_2$ is for the master integrals of section 3. Equation (25) contains none. On the line (13) this excludes the curve (16), its two images under permutations of the sites, and any other elliptic curve. The conclusion holds for every right factor of $\mathcal{L}_0$, so it does not depend on whether $\mathcal{L}_0$ is the operator of lowest order that annihilates V.

Three further results support this conclusion. When the same reduction is applied to a master integral of the elliptic sector, its operator has a second-order factor equivalent to $\mathcal{L}_2$, so the method

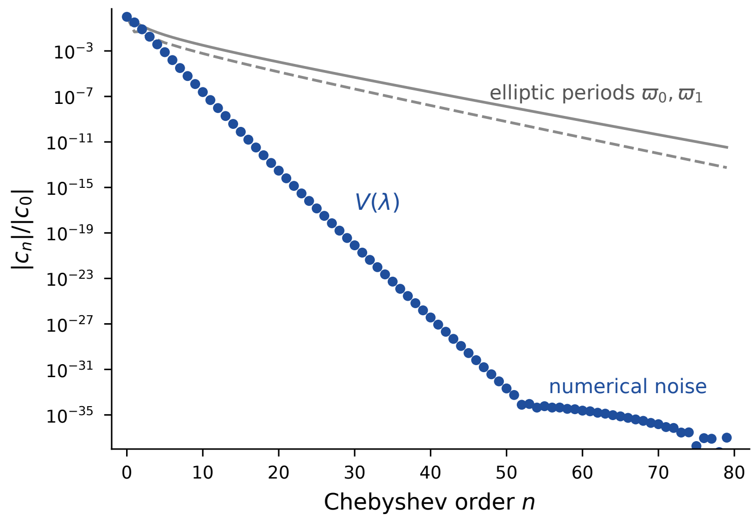

Figure 2: Chebyshev coefficients of the numerical values of $V(\lambda)$ on the interval $0.345 \le \lambda \le 0.985$, compared with those of the two elliptic periods ϖ_0 and ϖ_1 of eq. (19). The periods have logarithmic singularities at the ends of the physical interval, which limit the rate of decay. The coefficients of V decay at the rate set by the singular point $\lambda = 0$ until they reach the numerical noise.

detects the curve when it is present. A second reduction, which does not take the list of master integrals of section 3.1 as input, yields an operator of order 9 that divides $\mathcal{L}_0$ from the right and also annihilates V. Finally, the solutions of $\mathcal{L}_2$ have logarithmic singularities at $\lambda = \frac{1}{3}$ or at $\lambda = 1$, whereas the numerical values of V show no sign of a singularity at either point (figure 2). The closed form of section 4.4 makes the analyticity manifest.

4.4 The closed form

Once the function space is known, the coefficient itself can be found by the fitting procedure of appendix A, applied to the right space. We first solve $\mathcal{L}_0$ exactly. We make an ansatz in multiple polylogarithms $G(l_1, \ldots, l_w; \lambda)$ with letters $l_i \in \{0, \pm 1, \pm\frac{1}{3}\}$ and coefficients that are rational functions of λ. The equation $\mathcal{L}_0\, g = 0$ is linear in the unknown coefficients and can be solved in exact arithmetic. We find 5 solutions of weight zero, 19 of weight at most one and 20 of weight at most two. The count does not grow at weights three and four. The full solution space of $\mathcal{L}_0$ therefore consists of polylogarithms of weight at most two in these five letters, and the apparent singularities play no role.

The coefficient V is a combination of the 20 solutions with constant coefficients. We impose analyticity at $\lambda = 1$ exactly, fit the remaining constants to half of the numerical values of V, and identify them with an integer-relation algorithm as rational combinations of π^2, $\ln^2 2$ and 1. The result has a simple structure in terms of the site energies, which suggests its form for a general triangle. With one leg per site, for arbitrary momenta, we find

$$\int \mathrm{d}^3\ell\; \psi_3 \;=\; \frac{\pi}{q_{\mathcal{G}}} \left[\frac{\sum_i X_i \operatorname{Li}_2(u_i)}{\xi_1 \xi_2 \xi_3} + \frac{8\, X_1 X_2 X_3}{q_{\mathcal{G}}\, \xi_1^2 \xi_2^2 \xi_3^2}\, \mathcal{W} \right], \tag{26}$$

$$\mathcal{W} \;=\; \sum_i X_i\xi_i \operatorname{Li}_2(u_i) + 2\sum_{i<j} X_iX_j \,\ln(1-u_i)\ln(1-u_j) - \frac{\pi^2}{12}\sum_{i<j}\xi_i\xi_j\,, \qquad \xi_i = q_{\mathcal{G}} - 2X_i\,, \quad u_i = \frac{\xi_i}{q_{\mathcal{G}}}\,. \tag{27}$$

Figures 3 and 4 show the result. In the normalization of eq. (11), V is the right-hand side of eq. (26) multiplied by $q_{\mathcal{G}}/(4\sqrt{2})$. The variables ξ_i are positive by the triangle inequalities, and $\xi_i = 0$ is a degenerate triangle. The expression is finite there, because the bracket vanishes to second order. It is also finite when one of the momenta becomes soft.

On the line (13) the function space is exact, and the constants are recognized from numerical values. The formula then agrees with all numerical values of V on the line to their accuracy, which is better than 30 digits.

For general momenta we have no differential operator, and eq. (26) is an ansatz. The polynomial that multiplies each dilogarithm has degree four in the X_i and 9 undetermined rational coefficients. The polynomial that multiplies π^2 has degree five and 5 undetermined coefficients. We fitted these coefficients to numerical values of V. The same 14 numbers follow uniquely from the result on the line, so the fit is a test of the ansatz and not only of its coefficients. The formula agrees with the integral to 30 digits or better at generic, nearly degenerate and soft triangles that were not used in the fit. An analytic derivation of eq. (26), for instance by direct integration in the variables of section 2.3, would replace these numerical statements, and we leave it for future work.

To our knowledge the only earlier closed form for this coefficient is that of ref. [24], for the configuration in which one external momentum vanishes at arbitrary site energies. In that configuration the integration region degenerates to that of the two-site graph, and the result is again a combination of dilogarithms. Recent work has taken the coefficient at general momenta to be elliptic or hyperelliptic [16, 17]. Equation (26) makes the conclusion of this section explicit. With one leg per site, the one-loop triangle coefficient is a function of weight two with three dilogarithms, where we count the weight of the bracket in eq. (26) and not its overall factor of π, which is the complexity of a one-loop amplitude in flat space. Its structure indicates that the operator of lowest order that annihilates $V(\lambda)$ has order 7. We have not constructed this operator.

4.5 General site energies

The case of one leg per site is special. When $X_v = P_v$ the polynomial B becomes a perfect square at many of the points and lines where the factors (8) vanish together, and the corresponding square roots and curves degenerate. The site integrals of eq. (4) probe $X_v > P_v$, so it is important to know what happens there. We find that the coefficient remains a polylogarithmic function of weight two. Square roots appear in its arguments, and no elliptic period enters.

A second line. We first repeated the analysis of sections 4.2 and 4.3 on the line $X = P + \frac{1}{3}(1,1,1)$ with $P = (2\lambda, \lambda, 1)$. The structure of the master integrals is much richer than at $X = P$. There are 134 master integrals. Fifteen sectors in which two of the factors (8) vanish together contain an irreducible second-order block. Each block is equivalent to the Picard–Fuchs operator of the elliptic curve that B defines on the corresponding line. These sectors correspond to lines of the kind described in proposition 1, which we have matched to them by their denominators. At $X = P$ most of these curves degenerate.

The physical integrand avoids all of them. In the limit $\varepsilon \to 0$ the coefficient is a component of the solution of a first-order system of rank 44, $\mathrm{d}\vec{I} = M\vec{I}$. After a change of basis every entry of the matrix M is a sum of logarithmic forms $\mathrm{d}\ln(\,\cdot\,)$ with rational coefficients, whose arguments are rational or contain a single square root. No entry has a holomorphic or second-kind component on any of the elliptic curves, so the solution is an iterated integral of logarithmic forms. This is the analogue, for a system, of the factorization (25).

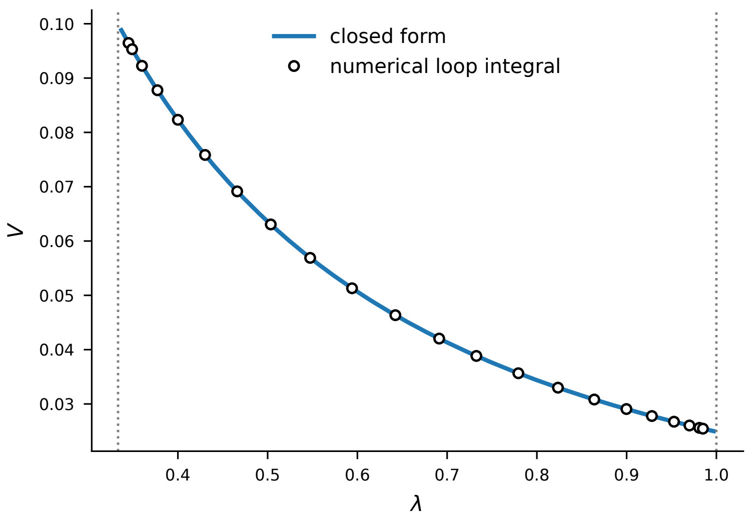

Figure 3: The coefficient V on the line (13). The line is the closed form (26) and the points are a subset of the numerical values. Over all 295 computed values the relative difference has median 5×10^{-34} and maximum 2×10^{-30}. The largest differences occur near $\lambda = 1$, where the numerical values are least accurate. The dotted lines mark the ends of the physical interval.

On this line the coefficient is a sum of ten terms, each a weight-two iterated integral divided by a square root. The ten square roots are the values of B at the four classes of points where three of the factors (8) vanish, and the leading coefficients of B on six lines where two of them vanish. All ten are perfect squares at $X = P$. The same analysis at $X = P$ reproduces the symbol of eq. (26) exactly.

The symbol in general kinematics. This structure determines the coefficient in general kinematics. We use the language of symbols [25]. The symbol of a function of weight two is a sum of ordered pairs of letters. The first entry of a pair records where the function has branch points, and a sum of pairs is the symbol of a function only if it satisfies an integrability condition. We consider functions of weight two whose symbols have the positive sums of energies as first entries,

$$q_{\mathcal{G}}\,, \quad X_i + P_i\,, \quad X_i + X_j + P_k\,, \quad X_i + P_j + P_k\,, \quad P_1 + P_2 + P_3\,. \tag{28}$$

The second entries are the letters that contain one of the ten square roots, and the symbol is odd under the change of sign of that root. For each of the ten square roots there is exactly one integrable symbol of this kind. With the smaller set of first entries $q_{\mathcal{G}}$, $X_i + P_i$ and $X_i + X_j + P_k$ there is none. The coefficient is therefore fixed up to ten rational numbers,

$$V(X;P) \;=\; \frac{\sqrt{2}\,\pi}{8}\,\mathrm{Re}\bigg[-\frac{1}{4}\,\frac{q_{\mathcal{G}}}{\sqrt{R_0}}\,F_0 - \frac{1}{2}\sum_{e}\frac{q_{\mathcal{G}}}{\sqrt{R_e}}\,F_e - \sum_{i<j}\frac{\rho^-_{ij}}{\sqrt{T^-_{ij}}}\,F^-_{ij} + \sum_{i<j}\frac{\rho^+_{ij}}{\sqrt{T^+_{ij}}}\,F^+_{ij}\bigg]\,, \tag{29}$$

where we have already inserted the values of the ten numbers. Here R_0 is $-2B$ evaluated at the point where the three subgraph energies of the sites vanish. The three R_e are $-2B$ at the points where $q_{\mathcal{G}} + 2y_e$ and the energies of the two sites at the ends of e vanish. The other radicands and prefactors are

$$\begin{aligned} T^{\pm}_{ij} &= \kappa(P) + 4P_i^2X_j^2 + 4P_j^2X_i^2 \pm 4X_iX_j\big(P_i^2 + P_j^2 - P_k^2\big)\,, \\ \rho^+_{ij} &= \frac{X_k}{X_i + X_j - X_k}\,, \qquad \rho^-_{ij} = \frac{X_k\,q_{\mathcal{G}}}{(X_i - X_j)^2 - X_k^2}\,, \end{aligned} \tag{30}$$

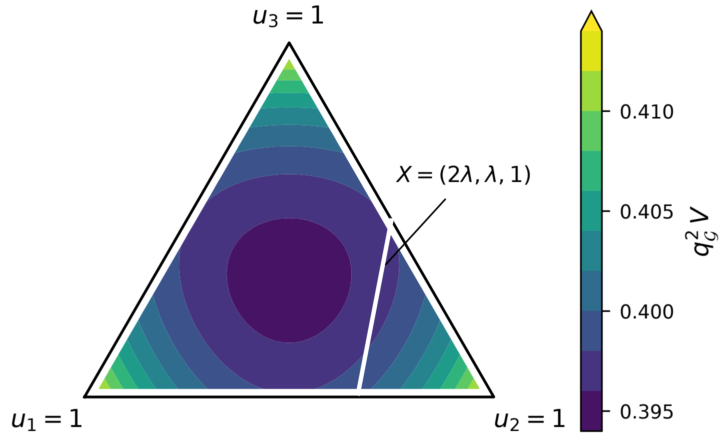

Figure 4: The closed form (26) for all triangles of momenta, in the variables $u_i = (q_{\mathcal{G}} - 2X_i)/q_{\mathcal{G}}$, which are positive and sum to one. The corners are soft limits and the edges are degenerate triangles. The combination $q_{\mathcal{G}}^2\, V$ varies only between 0.395 for the equilateral triangle and 0.417 in the soft limits. The white line is the line (13).

where $\kappa(P)$ is the Källén function of the P_v^2 and k is the third site.

The four functions. Each F is an explicit combination of dilogarithms whose arguments are of the form $(p + \sqrt{\cdot})/(p - \sqrt{\cdot})$ with p a polynomial in the energies. The functions $F_{ij}^{\pm}$ are sums of five and four functions of Bloch–Wigner type, $\mathrm{Li}_2(x) - \mathrm{Li}_2(\bar{x}) + \frac{1}{2}\ln(x\bar{x})\ln\frac{1-x}{1-\bar{x}}$, in which $x\bar{x}$ and $(1-x)(1-\bar{x})$ are rational in the energies.

The functions F_0 and F_e have a geometric structure. At a point where three of the factors (8) vanish, the P_v and the values of the y_e are the six edge lengths of a flat tetrahedron, with the convention that a negative y_e is a negative length. Let f_k be the perimeters of its four faces and c_j the perimeters of the three closed paths through all four vertices. Then

$$q(h) \;=\; \prod_{k=1}^{4}(h - f_k) \;-\; h\prod_{j=1}^{3}(h - c_j) \tag{31}$$

is a quadratic polynomial in h, and its discriminant is the radicand, $R = -2\det(\text{Cayley–Menger})$. Let $h_\pm$ be the roots of q, and let $\mathcal{B}(a)$ be the function of Bloch–Wigner type given above with arguments $1 - a/h_-$ and $1 - a/h_+$. Then

$$F_0 \;=\; -2\Big[\sum_{k=1}^{4}\mathcal{B}(f_k) - \sum_{j=1}^{3}\mathcal{B}(c_j)\Big]. \tag{32}$$

The symbol of F_0 pairs each face perimeter with the dihedral angles at the opposite vertex, and each path perimeter with the dihedral angles along the path. When $R < 0$ each term of eq. (32) is proportional to the volume of an ideal hyperbolic tetrahedron. The function F_e is a sum of nine terms of the same type, built from the tetrahedron at the corresponding point and from its image under $y_e \to -y_e$. We have not found a form with fewer terms, and within the class of arguments that we searched there is none. The permutations of the sites relate the three F_e, the three F_{ij}^{+} and the three F_{ij}^{-} to each other, so there are four independent functions. We give them in the ancillary files together with a numerical implementation. There is no term without a square root and no additive constant.

Status. The status of eq. (29) is the same as that of eq. (26). The count of one symbol for each square root is an exact computation at sampled kinematic points. It assumes the first entries (28), which we read off from the result on the line. The ten rational numbers were obtained from a fit to numerical values of V. With these numbers, eq. (29) agrees with the integral to more than 40 digits at all points with $X_v \geq P_v$ that were not used in the fit. These include near-degenerate triangles, soft momenta, and points close to $X = P$, where eq. (29) tends to eq. (26) (figure 5). A space of functions with rational letters only does not reproduce the values. At $X = P$ the ten square roots become rational, and the symbol of eq. (29) reduces exactly to that of eq. (26).

The ten numbers can also be obtained without a fit. On the line $X = P + \frac{1}{3}(1,1,1)$, the comparison of the ten symbols with the exact symbol of the first-order system fixes all ten, to the values shown, together with the relative normalization of the terms of lower weight. One overall constant remains numerical.

Region of validity. As written, with principal branches, the representation in terms of dilogarithms is valid for $X_v \geq P_v > 0$. Individual terms are singular where the prefactors (30) have poles, where a radicand vanishes, and where $P_k = |X_i - X_j|$. The sum has a finite limit there, and at $X = P$ it is given by eq. (26). The dilogarithms and square roots are evaluated on their principal branches and the real part is taken. We have tested this prescription throughout $X_v \geq P_v$, including points where a radicand is negative.

The coefficient itself is defined for all $X_v > 0$, and its integrand has no singularity there. Equation (29) continues to this whole region. For a negative radicand the corresponding term is a combination of Bloch–Wigner or Clausen functions. For a positive radicand it is the real form minus an integer multiple of $\pi^2/2$. The integer is fixed by analytic continuation along the ray $P \to tP$ from $t = 0$, where $X_v > P_v$. No numerical input enters. The continued expression agrees with the integral to the accuracy of the numerical values, and it is smooth across $X_v = P_v$ (figure 5). The ancillary files contain an implementation.

We conclude that the one-loop triangle coefficient is a polylogarithmic function of weight two for all positive site energies. The elliptic curves of its master integrals, three at $X = P$ and many more away from it, do not enter. The square roots do enter, and away from one leg per site the alphabet of the coefficient is algebraic.

5 Correlators

In this section we turn from the wavefunction coefficient to the equal-time correlator. The factors $q_{\mathcal{G}} + 2y_e$, on which the elliptic curve of section 3 sits, are known to be absent from correlators [18, 19].

The relative simplicity of correlators has been studied from several directions [26–28]. Ref. [9] pointed this out in connection with the elliptic sector and asked whether the correlator still requires elliptic functions. We give a short derivation of the cancellation from the recursion relations and explain where it comes from. We then ask what remains in the correlator integrand. All statements in this section concern integrands at fixed loop momentum.

5.1 The correlator integrand

The Born rule (2) expresses a correlator through products of wavefunction coefficients. At one loop the boundary profile of the field that runs around the loop is integrated over as well. With the Gaussian weight $|\Psi|^2$, this integral glues pairs of boundary legs of energy y_e together with a factor

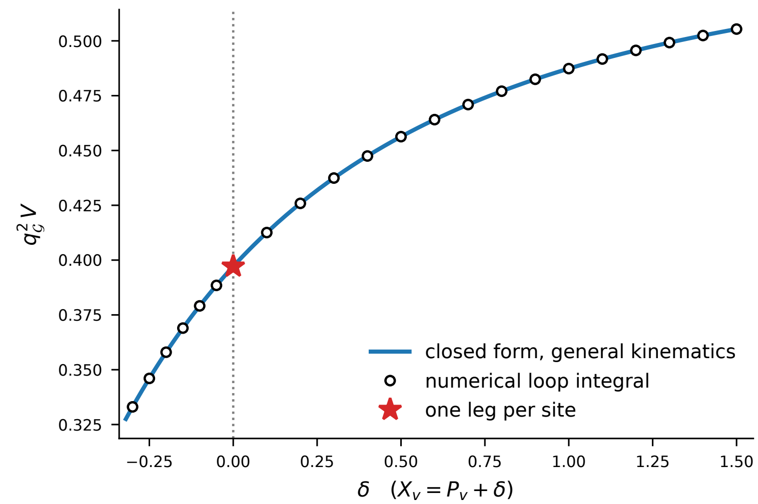

Figure 5: The coefficient through the case of one leg per site, for $P = (\frac{7}{5}, \frac{7}{10}, 1)$ and $X_v = P_v + \delta$. The line is eq. (29), continued to $\delta < 0$ as described in the text. The star is eq. (26) at $\delta = 0$, and the points are a direct numerical evaluation of the loop integral. The coefficient is continuous with no visible feature at $\delta = 0$, where all ten square roots of eq. (29) become rational.

$1/(2y_e)$. The correlator integrand of a graph G is therefore a sum over the sets of edges that are opened up into such pairs of legs. To state it compactly we strip the propagator prefactors and write $\hat{\psi}_G = \prod_e (2y_e)\, \psi_G$. For vertex factors that do not depend on time, the sum is

$$C_G \;=\; \sum_{S \subseteq \text{edges}} 2^{\,n(S)-1} \prod_{j=1}^{n(S)} \hat{\psi}_{H_j}\,, \tag{33}$$

where opening the edges in S leaves $n(S)$ connected components H_j. Each opened edge adds its energy y_e to the two sites at its ends. The correlator integrand is C_G divided by $\prod_e 2y_e$ and by factors that depend only on the external legs. The first terms of eq. (33) are the loop itself and the chains in which one edge is opened, and they enter with equal weight.

5.2 Cancellation of the factors $q_{\mathcal{G}} + 2y_e$

Consider the polygon with N sites, and write G_e for the chain obtained by opening the edge e. The terms of eq. (33) with poles at $q_{\mathcal{G}} + 2y_e = 0$ are the loop and the chains, which appear in the combination

$$\Phi_G \;=\; \hat{\psi}_G + \sum_e \hat{\psi}_{G_e}\,. \tag{34}$$

The recursion of ref. [3] gives $q_{\mathcal{G}}\, \hat{\psi}_G = \sum_e 2y_e\, \hat{\psi}_{G_e}$ for the loop. The total energy of the chain G_e is $q_{\mathcal{G}} + 2y_e$, so the same recursion gives $(q_{\mathcal{G}} + 2y_e)\, \hat{\psi}_{G_e} = \sum_{f \neq e} 2y_f\, \hat{\psi}_{G_e \setminus f}$. Here $G_e \setminus f$ is the pair of chains left after a second edge f is opened. We add the first relation to the sum of the second over e. The terms $2y_e \hat{\psi}_{G_e}$ cancel, and we find

$$q_{\mathcal{G}}\, \Phi_G \;=\; \sum_{e \neq f} 2y_f\, \hat{\psi}_{G_e \setminus f}\,. \tag{35}$$

The right-hand side contains only tree coefficients in which each site has received the energy of an opened edge at most once. Its poles are therefore subgraph energies of G, and the poles of $\hat{\psi}_G$ and of $\hat{\psi}_{G_e}$ at $q_{\mathcal{G}}+2y_e=0$ cancel in Φ_G. The remaining terms of eq. (33) have two or more edges opened and are of the same kind as the right-hand side. For the triangle one can check eq. (35) directly from eq. (7). The denominator of Φ_G consists of $q_{\mathcal{G}}$ and the six subgraph energies of eq. (8). The argument extends by induction to polygons with trees attached. Ref. [18] derives the cancellation in much greater generality, for any number of loops and any time dependence of the background, as a cosmological analogue of the Kinoshita–Lee–Nauenberg theorem.

Intuitively, the factors $q_{\mathcal{G}} + 2y_e$ belong to the boundary condition of the wavefunction and not to the time evolution. The propagator (5) is the sum of a time-ordered term and a factorized term, $e^{-y(t+t')}$, which makes fluctuations vanish on the late-time boundary. A factor that counts an edge twice requires both ends of the edge to deposit the energy $+y_e$ into the same set of sites. The time-ordered term deposits $+y_e$ at its earlier end only, so the factors $q_{\mathcal{G}} + 2y_e$ come from the factorized term. In the correlator the integral over boundary profiles produces the chains G_e, in which the edge is replaced by the same pair of boundary legs. The two contributions cancel. The elliptic curve of section 3 is in this sense a feature of conditioning on the boundary profile.

5.3 What remains in the correlator

The cancellation removes the curve of section 3 from the correlator integrand of the triangle. We have also looked for elliptic curves on the other singular loci of the integrand. The most singular loci are the lines in the space of edge energies on which two denominator factors vanish. On such a line the measure restricts to the square root of a polynomial of degree at most four. The question is whether the polynomial defines an elliptic curve and whether the integrand has a residue there. For the triangle, proposition 1 shows that the lines on which the polynomial defines an elliptic curve, which we call elliptic lines, are exactly those that lie in one of the planes $q_{\mathcal{G}} + 2y_e = 0$. The correlator integrand has no pole on these planes, so it has no residue on any elliptic line. The wavefunction integrand has residues on 12 of them, and by proposition 1 these residues involve no elliptic period. For the triangle the elliptic curves are therefore invisible both to the correlator and to the physical wavefunction integrand, for different reasons.

We have repeated the analysis for the box and the pentagon in the dimension $d = N$. In this dimension the N edge energies are independent coordinates on the space of loop momenta, and the measure is again the inverse square root of a Cayley–Menger polynomial, now that of the simplex with $N+1$ vertices. For the triangle this dimension is the physical one. Their wavefunction integrands have residues on elliptic lines, including lines on which only subgraph energies vanish, and their correlator integrands have none. We have not studied singular loci of higher dimension. When the exponent of B is an integer, as for the box in $d = 3$, the relevant curves are of a different kind, and some of them do have residues in the correlator integrand. We leave these cases open.

Two further checks concern graphs and backgrounds beyond those of this paper. With vertex factors $(-\eta)^{-(1+\sigma)}$ the weights in eq. (33) acquire a phase for each connected component that depends on its number of sites. The loop and the chains G_e have the same sites, so Φ_G is unchanged, and the site integrals of eq. (4) act on it as a whole. For the triangle we have verified numerically that the site-integrated wavefunction coefficient has a branch point at $q_{\mathcal{G}} + 2y_{12} = 0$ and the correlator integrand does not. The test used three values of $\sigma < 0$ and an analytic continuation to $\sigma = 0.3$. At two loops we have examined the sunrise, the kite and five other graphs with up to four sites. In each of them every factor that counts an edge more than once is absent from the correlator integrand, in agreement with ref. [18]. Whether a two-loop correlator with generic site energies has an elliptic singular locus is open.

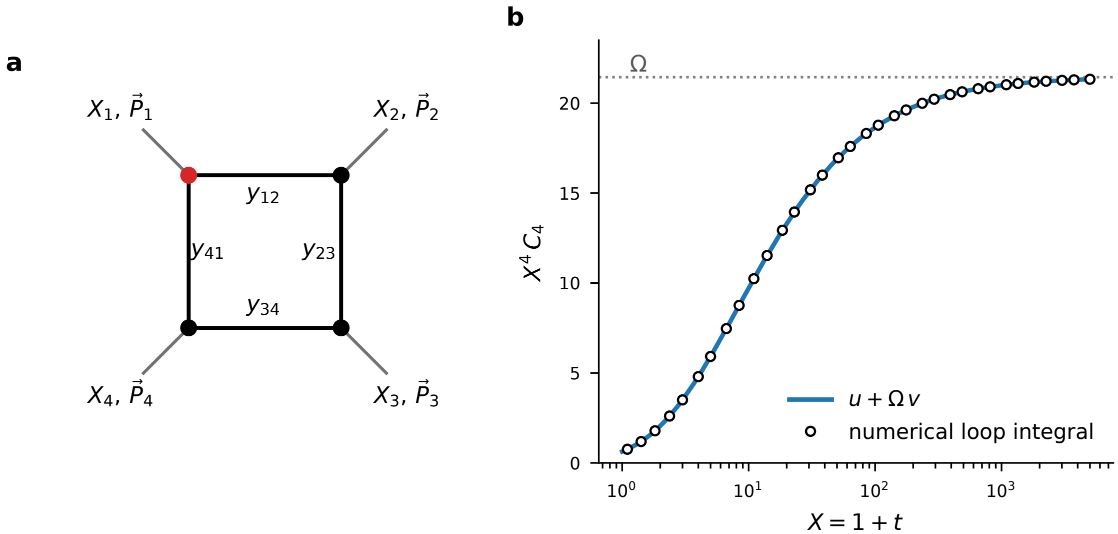

Figure 6: (a) The one-loop box. Each site carries the energy X_v and the momentum $\vec{P}_v$ of its external legs. The pole of site 1, marked in red, is the one on which the residue (36) has two square roots. (b) The correlator on the line of section 6.5, multiplied by X^4. The line is eq. (42) and the points are direct numerical values of the loop integral. The dotted line is the constant Ω, which the curve approaches at large X.

6 The box

The mechanism of proposition 1 is special to the triangle. In this section we show where it fails for the one-loop graph with four sites, shown in figure 6(a). We then give the simplest discontinuity of the box in closed form, and it is an elliptic function. We use the notation of section 2, with sites $v = 1, \ldots, 4$, edge energies y_{12}, y_{23}, y_{34} and y_{41}, and the loop-integrated coefficient $V_4 = \int \mathrm{d}^3\ell\, \psi_4$.

6.1 The pole of a single site

For the triangle the elliptic curve was attached to the factors $q_{\mathcal{G}} + 2y_e$. For the box the residue on these factors is again a flat-space amplitude, which depends on the remaining edge energies only through their squares. The factors that contain two or three sites are also harmless. The obstruction comes from the simplest factor of all, the energy of a single site. On the pole $X_1 + y_{41} + y_{12} = 0$ the residue of the integrand is

$$\operatorname*{Res}_{X_1 = -y_{41} - y_{12}} \psi_4 \;=\; \frac{1}{4\, y_{12}\, y_{41}} \sum_{s, s' = \pm 1} s\, s'\, \psi_{\text{chain}}\big(X_2 + s\, y_{12}\,,\; X_3\,,\; X_4 + s'\, y_{41}\,;\; y_{23}\,,\; y_{34}\big)\,, \tag{36}$$

where ψ_{chain} is the tree-level coefficient of the chain of the three remaining sites,

$$\psi_{\text{chain}}(X_2, X_3, X_4; y, y') \;=\; \frac{(X_2 + X_3 + y')^{-1} + (X_3 + X_4 + y)^{-1}}{(X_2 + X_3 + X_4)(X_2 + y)(X_3 + y + y')(X_4 + y')}\,. \tag{37}$$

The residue is even in y_{12} and in y_{41}. It is not even in y_{23} or in y_{34}, the energies of the two edges that do not end on site 1. The same formula holds for every polygon, with the chain of the remaining sites in place of eq. (37).

This explains the difference between the triangle and the box. On the pole the loop momentum lies on a spheroid with foci at the two points where y_{12} and y_{41} vanish. Each of the other edge energies is the square root of a quadratic function on this surface. The triangle has one such edge, and a single square root of a quadratic can be rationalized. The box has two. Along a line on the spheroid the two roots define the curve $Y^2 = q_{23}\, q_{34}$, where $q_e = y_e^2$ is quadratic in the coordinate along the line. This curve has genus one. For the pentagon the three roots give a curve of genus five.

6.2 One leg per site

With one leg per site, $X_v = P_v$, the structure of the single-site pole becomes one-dimensional. The discontinuity of V_4 across the cut that starts at $X_1 = -P_1$ is the integral of the residue (36) over the spheroid $y_{41} + y_{12} = -X_1$. At the threshold the spheroid collapses onto the segment between its foci. We parametrize the segment by $d = y_{41} - y_{12}$ with $-P_1 \le d \le P_1$. On it

$$y_{23}^2 \;=\; \frac{(P_1+d)\,P_2^2 + (P_1-d)\,P_{12}^2}{2P_1} - \frac{P_1^2-d^2}{4}\,, \qquad y_{34}^2 \;=\; \frac{(P_1+d)\,P_{41}^2 + (P_1-d)\,P_4^2}{2P_1} - \frac{P_1^2-d^2}{4}\,, \tag{38}$$

with $P_{12} = |\vec{P}_1 + \vec{P}_2|$ and $P_{41} = |\vec{P}_4 + \vec{P}_1|$. We define the threshold value of the discontinuity as

$$D_0 \;=\; \frac{\pi}{4P_1} \int_{-P_1}^{P_1} \mathrm{d}d \sum_{s,s'=\pm1} s\, s'\; \psi_{\rm chain}\Big(P_2 + s\,\tfrac{P_1-d}{2}\,,\; P_3\,,\; P_4 + s'\,\tfrac{P_1+d}{2}\,;\; y_{23}\,,\, y_{34}\Big)\,. \tag{39}$$

For momenta that do not lie in a plane the four roots of $y_{23}^2\, y_{34}^2$ are distinct and complex, and eq. (39) is an integral on an elliptic curve. Its j-invariant depends on the shape of the quadrilateral formed by the momenta.

The quantity D_0 is a piece of the physical coefficient. When the momentum of the leg at site 1 becomes soft, the coefficient with one leg per site behaves as

$$V_4 \;=\; -D_0\, \log 2P_1 \;+\; \text{terms analytic at } P_1 = 0\,. \tag{40}$$

We have verified this numerically for two quadrilaterals that do not lie in a plane.

The integral (39) can be done in closed form. The integrand is a rational function of d, y_{23} and y_{34} with simple poles. Partial fractions reduce it to logarithms and to the integrals of the first and third kind on the curve $s^2 = 16\, y_{23}^2\, y_{34}^2$. The result has the structure

$$D_0 \;=\; \frac{\pi}{4P_1}\Big[\,\frac{1}{4}\sum_{\text{poles}} \rho\,\big(L_0 + \eta\, L_{23} + \eta' L_{34} + \eta\,\eta'\, L_\Pi\big) \;+\; 4\, p_0\, J_F\Big]\,, \qquad J_F = \int_{-P_1}^{P_1} \frac{\mathrm{d}d}{s} = 2R_F\,, \tag{41}$$

where L_0, L_{23} and L_{34} are logarithms and L_Π is a combination of the Carlson integrals R_F and R_J and a logarithm. The sum runs over the poles of the integrand on the four sheets $(\eta, \eta') = (\pm y_{23}, \pm y_{34})$ of the two roots, and the coefficients ρ and p_0 are algebraic functions of the six lengths in eqs. (38) and (39). We derive the complete expressions in appendix B.3, and the ancillary files contain an evaluator. The coefficient p_0 of the integral of the first kind does not vanish. Figure 7 compares eq. (41) with a numerical integration of eq. (39). For momenta in a plane one of the poles becomes a double pole, and eq. (41) requires an additional term that we have not included.

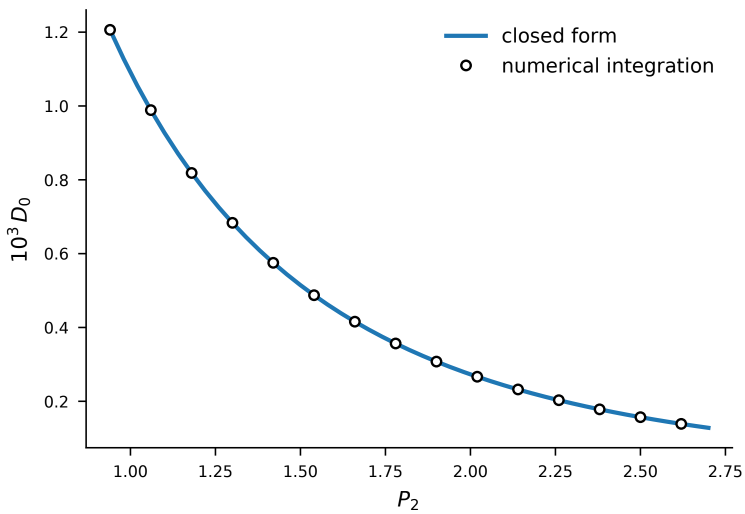

Figure 7: The threshold discontinuity D_0 of the box with one leg per site, for $P_1 = 1$, $P_3 = 2$, $P_4 = \frac{7}{4}$, $P_{12} = \frac{9}{5}$ and $P_{41} = 2$, as a function of P_2. The line is the closed form (41) and the points are numerical values of the integral (39). The two agree to better than 10^{-33} at all 45 points computed.

6.3 The box is not polylogarithmic

An elliptic integral in a discontinuity does not by itself exclude a polylogarithmic answer, as the triangle shows. For the box, two tests show that the curve survives. The first concerns the function D_0. We continue it analytically in one of the lengths of the quadrilateral, around the points where the curve degenerates. The monodromy contains elements with integer traces larger than two, whose eigenvalues are not roots of unity. Iterated integrals of logarithmic forms with algebraic letters have quasi-unipotent monodromy, so D_0 is not of this type. The triangle, taken through the same computation, gives unipotent monodromy.

The second test is exact and concerns the integrand. The residue (36) generates a differential module as the shape of the quadrilateral varies. At one leg per site this module contains the periods of the curve $Y^2 = q_{23}\, q_{34}$. A logarithmic form on the same curve generates a module that does not contain them. For the triangle the corresponding curve is a conic and has no periods.

The first test is numerical and acts on the function, and the second is exact and acts on the class of the residue. Together with eq. (40) they show that the box with one leg per site is elliptic, in the sense that the periods of an elliptic curve enter its soft limit. The triangle is the last polygon of this theory that is polylogarithmic.

6.4 Beyond the threshold

Above the threshold the spheroid no longer collapses. The discontinuity is then an integral over the double cover of the spheroid defined by the two roots, which is a K3 surface fibred by elliptic curves. Its periods obey a differential equation in $y_{41} + y_{12}$. The order is five when the momenta form a regular tetrahedron, six for a less symmetric family, and eight for generic momenta. At the symmetric point we have the operator exactly. It is not a symmetric power of a second-order operator, so its solutions are not products of elliptic periods. The five solutions obey one quadratic relation with constant coefficients, as the periods of a K3 surface must.

The physical integrand couples to these periods. With several legs per site the leading term of the residue at large site energies generates the full fifth-order block, so the box is a function of K3 type. At exactly one leg per site we have two pieces of evidence. The block has square-root branch points at complex values of $y_{41} + y_{12}$, and the single-site discontinuity has the same branch points with the predicted coefficient. An exact reduction of the integrand, with regular-tetrahedron momenta and three site energies fixed at one leg per site, gives a module that contains the holomorphic form of the K3 surface. The same holds for the integrand of the correlator. We have not tested generic momenta. Appendix B gives the details.

6.5 The box on a line

On one line in kinematic space the box can be computed in the sense of section 4. We take momenta that form a regular tetrahedron of unit side and site energies $X_v = 1 + t$, so that $t = 0$ is the case of one leg per site. An integration-by-parts reduction with the regulator of eq. (11) gives exact first-order differential systems in t for the loop-integrated coefficient V_4 and for the corresponding correlator C_4. As for the triangle, the limit $\varepsilon \to 0$ must be taken with care, because the master integrals have double poles in ε. The coefficients of the double poles are residues at infinite loop momentum, and they do not depend on the kinematics. With this input the systems have dimension 28 for the correlator and 34 for the coefficient.

The systems determine the function space on the line. Their irreducible blocks are the fifth-order operator of section 6.4, the second-order operators of three elliptic curves, and first-order blocks with rational and square-root letters. The three curves are those on which two subgraph energies vanish. The curve of eq. (39) degenerates on this line and does not appear. The periods of the three curves are hypergeometric functions of their j-invariants, of the form $c_4^{-1/4}\,{}_2F_1(\frac{1}{12}, \frac{5}{12}; 1; 1728/j)$ with a polynomial $c_4(t)$. The elliptic blocks contribute to the physical functions. The monodromy of the solutions indicates that the fifth-order operator contributes as well, but we have not separated it from the first-order pieces of its block.

We have tested the systems against direct numerical values of both functions. A test of this kind needs care. A fit of all boundary constants to values on a short interval reproduces the values of any smooth function, so it decides nothing. The test becomes decisive with values close to the singular points and at large t, together with the conditions on the double poles. The solutions then predict the values that were not used in the fit, and the same fit to a different function fails. The solutions continue to $t = 0$, where they agree with a direct evaluation at one leg per site.

6.6 The correlator on the line

For the correlator the analysis can be carried to the end. With $X = 1 + t$ the result is

$$\begin{aligned} C_4(t) &= u(t) + \Omega\, v(t)\,, \\ \Omega &= \int \mathrm{d}^3\ell \, \frac{1}{y_{12}\, y_{23}\, y_{34}\, y_{41}} = 21.444429513935774519503166765342653 5\,, \end{aligned} \tag{42}$$

where u and v are two solutions of the system and Ω is a number. In the integral the four edge energies are the distances from $\vec{\ell}$ to the vertices of the regular tetrahedron. The value shown has a relative uncertainty of 5×10^{-34}. Figure 6 shows the result.

The functions u and v are fixed without reference to any value of C_4. The loop integral converges for $t > -1$, so the physical solution is single-valued around the singular points of the system in that range. The solutions that are single-valued around the six points listed in appendix B.6 form a space of dimension four. At large X the correlator has the expansion

$$C_4 \;=\; \sum_{n\geq 4} X^{-n}\big(\alpha_n + \beta_n \log X\big)\,, \qquad \alpha_4 = \Omega\,, \quad \beta_5 = -24\pi\,, \quad \beta_7 = -\tfrac{158}{3}\,\pi\,, \tag{43}$$

with $\beta_n = 0$ for even n. The expansion by regions gives these coefficients exactly. Exactly one solution in the four-dimensional space is free of logarithms at large X, and v is this solution, normalized to begin with X^{-4}. The exact coefficients then determine u. They do not constrain the coefficient of v, which is Ω. It is the only number in C_4 that the system and the exact data leave undetermined. We have found no integer relation between Ω and familiar constants.

The expression $u + \Omega\, v$ contains no fitted number, and it agrees with all direct numerical values of C_4 to their accuracy. It is a closed form in a weaker sense than eq. (29), because u and v are defined through a differential system and not through named functions. For the coefficient V_4 the same construction leaves two undetermined constants. We leave a basis of functions for v, and the reduction of V_4 to a single constant, for future work.

7 Discussion

The elliptic curve of the one-loop triangle is a property of its master integrals and not of the wavefunction coefficient. The coefficient is a polylogarithmic function of weight two for all positive site energies. This statement is exact on the two lines that we analysed, and elsewhere it rests on the agreement of eq. (29) with the integral. The reason is proposition 1. At the poles that carry the curve, the residue of the physical integrand is a flat-space amplitude, which has a single square root at most. The same reasoning shows where the simplification ends. For the box the residue at the pole of a single site has two square roots, and the periods of an elliptic curve and of a K3 surface enter both the coefficient and the correlator (section 6). The triangle is therefore the last polygon of this theory that is polylogarithmic.

These results concern the flat-space coefficient, which is the integrand of the site integrals (4). For a cubic interaction in de Sitter space the site integrals have a flat measure. They change the behaviour of the integrand at large loop momentum from ℓ^{-5} to $\zeta(3)/(8\ell^3)$, so the de Sitter coefficient has a late-time logarithm. The site integrals and the loop integral can then be exchanged only with a regulator. With one leg per site the rest of the momentum dependence is fixed by symmetry. At late times the coefficient is a three-point function of operators with $\Delta = 2$ in a three-dimensional conformal theory [29]. If a cutoff Λ on the comoving loop momentum breaks the symmetry only through the logarithm, then

$$\psi_3^{\mathrm{dS}} \;=\; \int^{\Lambda} \mathrm{d}^3\ell \int_0^{\infty} \mathrm{d}^3\omega\; \psi_3(X+\omega; y) \;=\; -\frac{\pi\,\zeta(3)}{2}\,\ln\frac{k_T}{\Lambda} + b\,, \qquad k_T = k_1 + k_2 + k_3\,, \tag{44}$$

where $k_v = P_v$ is the magnitude of the momentum of the leg at site v and b is a number. A direct evaluation at two kinematic points confirms this form. For the corresponding correlator the loop integral converges, and symmetry allows only a constant. Numerically the constant is $-3\pi^2\zeta(3)$. With one leg per site the de Sitter triangle is therefore a logarithm and two numbers, whatever functions appear in V. The function class of the flat-space coefficient matters when several legs meet at a site, or when the external legs break the de Sitter boosts. In those cases the de Sitter and power-law coefficients are integrals of eq. (29) over the site energies. Whether these integrals remain polylogarithmic, and whether the ten square roots can be rationalized simultaneously, are natural next questions.

Several steps of our analysis ask for a derivation. Equations (26) and (29) were found by fixing the function space exactly and a small number of rational constants numerically. The ten constants of eq. (29) are $-\frac{1}{4}$, $-\frac{1}{2}$ and ± 1, which suggests that a direct derivation exists. It might also lead to a form that is manifestly analytic across $X_v = P_v$. For the box the open problems are of a different kind. The correlator on one line is known up to the single number Ω of eq. (42), but its two building blocks are defined through a differential system and not through named functions. The coefficient on the same line still contains two undetermined constants, and we have not treated generic momenta, for which the period block of the K3 surface has order eight. For the pentagon the residue at the pole of a single site involves three square roots and a curve of genus five, and we have not examined it further. We have also not gone beyond one loop. In the two-loop graphs that we examined, the correlator integrand contains subgraph energies only.

For the triangle two facts stand side by side. The curve of the master integrals is attached to a factor that the correlator does not contain, and the curve also cancels in the wavefunction coefficient. Both trace back to the factorized term of the propagator (5), but we do not have a general argument that relates them. The box shows that neither fact is general, since there the curves sit on poles of subgraph energies, which the correlator shares. A formulation in terms of the cosmological polytope, in which the physical integrand is a canonical form and the master integrals are not, may explain when the geometry of the master integrals overestimates the function space.

All fields in this paper are conformally coupled, so that the integrand is a rational function. For fields of general mass the singular loci of the integrand are the same, but the integrand is no longer rational, and the methods used here do not apply directly. The leading signals of a triangle loop of massive fields have recently been obtained with cutting rules [30], and one-loop signals of this kind can be integrated numerically [31]. The function class of such loops is an open problem.

A Derivation of the closed form

In this appendix we derive the closed form (26). We first describe how the operator $\mathcal{L}_0$ is obtained and how it is tested against the integral. We then construct its solutions, select the solution that equals V on the line (13), and extend the result to a general triangle. We end with the limits of the closed form and with a comparison of the method with other bootstrap methods in cosmology.

A.1 The operator and its singular points

The integration-by-parts identities of the family (14) follow from the vector fields that preserve B up to a factor. We solve them by linear algebra modulo prime numbers at numerical values of λ and ε. Modulo these identities, the integrand of V and its derivatives with respect to λ span a space of finite dimension, so that they obey a linear relation, which is the differential operator. We reconstruct its coefficients as rational functions of λ from sample points, and we lift them to the rational numbers with the Chinese remainder theorem.

The operator $\mathcal{L}_0$ of eq. (24) has singular points at $\lambda = 0$, $\pm\frac{1}{3}$ and ± 1 and at infinity, and its local exponents are integers at each of them. The other zeros of its leading coefficient are apparent singularities, at which every solution is analytic. On the line (13) the singular points are the zeros of the variables of eq. (27),

$$q_{\mathcal{G}} = 3\lambda + 1\,, \qquad \xi_1 = 1 - \lambda\,, \qquad \xi_2 = 1 + \lambda\,, \qquad \xi_3 = 3\lambda - 1\,, \qquad X_2 = \lambda\,. \tag{45}$$

The points $\lambda = 1$ and $\lambda = \frac{1}{3}$ are the two degenerate triangles at the ends of the physical interval, and $\lambda = 0$ is the limit in which two of the momenta become soft. The points $\lambda = -\frac{1}{3}$ and $\lambda = -1$ lie outside the physical region.

We test $\mathcal{L}_0$ against numerical values of V without differentiating them. The values are obtained from eq. (11) at $\varepsilon = 0$. The integral over y_{12} can be done in closed form, and we evaluate the remaining two-dimensional integral with double-exponential quadrature to 33 to 35 digits. Let φ be a function on an interval $a \le \lambda \le b$ that vanishes at both ends together with its first 19 derivatives. Integration by parts then moves all derivatives from V to φ without boundary terms,

$$\int_a^b \varphi\,\mathcal{L}_0 V\,\mathrm{d}\lambda \;=\; \int_a^b V\,\mathcal{L}_0^\dagger\varphi\,\mathrm{d}\lambda\,, \qquad \mathcal{L}_0^\dagger\varphi \;=\; \sum_{i=0}^{20}(-1)^i\,\frac{\mathrm{d}^i}{\mathrm{d}\lambda^i}\big(c_i\,\varphi\big)\,. \tag{46}$$

The right-hand side contains only the values of V, and it vanishes for every such φ if $\mathcal{L}_0 V = 0$. We take $\varphi_m = [(\lambda-a)(b-\lambda)]^{20} P_m$, where P_m is the Legendre polynomial of degree m on the interval. For $\mathcal{L}_0$ the integrals vanish to the accuracy of the numerical values. For the operator of order 14 they do not.

A.2 The space of solutions

We now construct all solutions of $\mathcal{L}_0$. Since the singular points are 0, $\pm\frac{1}{3}$ and ± 1, we look for solutions among the multiple polylogarithms with these five letters. They are defined recursively by $G(;\lambda) = 1$ and

$$\frac{\mathrm{d}}{\mathrm{d}\lambda}\,G(a,w;\lambda) \;=\; \frac{G(w;\lambda)}{\lambda-a}\,, \tag{47}$$

where a is a letter and w is a word in the letters, and the number of letters of a word is its weight. We make the ansatz

$$F(\lambda) \;=\; \sum_w R_w(\lambda)\,G(w;\lambda)\,, \tag{48}$$

where the R_w are rational functions of λ and the sum runs over all words up to a given weight. To apply $\mathcal{L}_0$ to the ansatz we use the behaviour of the multiple polylogarithms under a shift of the argument,

$$G(w;\lambda+\tau) \;=\; \sum_{w=\pi\sigma} h_\pi(\tau)\,G(\sigma;\lambda)\,, \tag{49}$$

where the sum runs over all ways to split the word w into a first part π and a second part σ. The function $h_\pi(\tau)$ is the iterated integral of the word π along the segment from λ to $\lambda+\tau$, and it is a power series in τ with rational coefficients. Since the i-th derivative of F is $i!$ times the coefficient of τ^i in $F(\lambda+\tau)$, we obtain

$$\mathcal{L}_0 F \;=\; \sum_\sigma G(\sigma;\lambda)\,\sum_{i=0}^{20} c_i\; i!\;\big[\tau^i\big]\sum_\pi R_{\pi\sigma}(\lambda+\tau)\,h_\pi(\tau)\,. \tag{50}$$

The multiple polylogarithms are linearly independent over the rational functions, so that the coefficient of each $G(\sigma;\lambda)$ must vanish. The term with empty π is $\mathcal{L}_0 R_\sigma$, and the other terms contain only the coefficients of words that are longer than σ. The coefficients of the longest words are therefore rational solutions of $\mathcal{L}_0$. The equations for the shorter words are linear equations for rational functions, which we solve in exact arithmetic, starting from the highest weight.

We find 5 rational solutions, 14 further solutions of weight one and one solution of weight two. No further solutions appear when we admit words of weight three and four. Since $\mathcal{L}_0$ has order 20, these are all of its solutions. In particular the apparent singularities do not contribute letters.

A.3 The coefficient on the line

The coefficient V is a combination of the 20 solutions with constant coefficients. We fix the constants in two steps. First, the integral (11) is analytic at the degenerate triangle $\lambda = 1$. The solutions of $\mathcal{L}_0$ that are analytic at $\lambda = 1$ form a subspace of dimension 14, which we determine exactly. Second, we fit the 14 constants of this subspace to numerical values of V at half of the points at which we have computed it. The ratios among ten of the constants are rational numbers, which we read off from the fit. We identify the remaining constants with an integer-relation algorithm, in the manner that is standard for multiloop amplitudes [20]. They are combinations of π^2 and $\ln^2 2$ with rational coefficients, multiplied by an overall factor of $\sqrt{2}\,\pi$. The logarithms of 2 come from the choice of base point and cancel in the final result. We accept the result because it reproduces the values that were not used in the fit.

All multiple polylogarithms of weight two in the result combine into the three dilogarithms $\mathrm{Li}_2(u_i)$ and into products of the logarithms $\ln(1-u_i) = \ln(2X_i/q_{\mathcal{G}})$. With the variables of eq. (45) we obtain

$$
\begin{aligned}
\frac{q_{\mathcal{G}}^2\,\xi_1^2\,\xi_2^2\,\xi_3^2}{\pi} \int \mathrm{d}^3\ell\ \psi_3 \ &= \ 2\lambda(1-\lambda)\,p_1\,\mathrm{Li}_2(u_1) + \lambda(1+\lambda)\,p_2\,\mathrm{Li}_2(u_2) \\
&\quad + (3\lambda-1)\,p_3\,\mathrm{Li}_2(u_3) + \frac{4\pi^2}{3}\,\lambda^2\big(\lambda^2 - 6\lambda + 1\big) \\
&\quad + 32\lambda^3\big[\,2\lambda\,\ell_1\ell_2 + 2\,\ell_1\ell_3 + \ell_2\ell_3\big]\,,
\end{aligned}
\tag{51}
$$

where $\ell_i = \ln(1-u_i)$ and the three polynomials are

$$
p_1 = 9\lambda^3 + 25\lambda^2 - \lambda - 1\,, \qquad p_2 = -9\lambda^3 + 25\lambda^2 + \lambda - 1\,, \qquad p_3 = -3\lambda^3 + 15\lambda^2 + 3\lambda + 1\,. \tag{52}
$$

The right-hand side of eq. (51) vanishes to second order at $\lambda = 1$ and at $\lambda = \frac{1}{3}$, so that V is finite at both ends of the physical interval.

A.4 General triangles

For general momenta we have no differential operator, and we infer the result from the structure of eq. (51). Each of its terms has a simple form in the site energies $X = (2\lambda, \lambda, 1)$. The prefactors of the dilogarithms are $X_i\,\xi_i$, and the three polynomials are one symmetric expression,

$$
p_i \ = \ q_{\mathcal{G}}\,\xi_j\,\xi_k + 8X_1X_2X_3\,, \tag{53}
$$

where i, j and k are distinct. For example $q_{\mathcal{G}}\,\xi_2\,\xi_3 + 8X_1X_2X_3 = (3\lambda+1)(1+\lambda)(3\lambda-1) + 16\lambda^2$, which is p_1. The coefficient of $\ell_i\,\ell_j$ is $16\,X_1X_2X_3\,X_iX_j$. This suggests the ansatz

$$
\begin{aligned}
\frac{q_{\mathcal{G}}^2\,\xi_1^2\,\xi_2^2\,\xi_3^2}{\pi} \int \mathrm{d}^3\ell\ \psi_3 \ &= \ -\sum_i \xi_i\, b(X_i; X_j, X_k)\,\mathrm{Li}_2(u_i) + \pi^2\, c(X) \\
&\quad + 16\,X_1X_2X_3 \sum_{i<j} X_iX_j\,\ell_i\,\ell_j
\end{aligned}
\tag{54}
$$

for an arbitrary triangle. Here $b(u;v,w)$ is a homogeneous polynomial of degree four that is symmetric in v and w, and c is a symmetric homogeneous polynomial of degree five. The polynomial b has 9 coefficients and c has 5. We restrict eq. (54) to the line and compare it with eq. (51). The three dilogarithms are linearly independent over the rational functions of λ, so that the coefficient of each of them must agree as a polynomial in λ. This gives linear equations for the coefficients of b and c. Their unique solution is

$$b(u;v,w) \;=\; -u\left[(u+v+w)(u-v+w)(u+v-w)+8\,u\,v\,w\right], \qquad c(X) \;=\; -\frac{2}{3}\,X_1X_2X_3\sum_{i<j}\xi_i\,\xi_j\,. \tag{55}$$

With these polynomials eq. (54) becomes eq. (26).

The line determines the 14 coefficients, but it does not test the form of the ansatz. We therefore compare eq. (26) with numerical values of the integral at triangles away from the line. A fit of the 14 coefficients to such values returns the numbers of eq. (55), and the formula agrees with the integral to better than 34 digits at 21 generic triangles that were not used in the fit. At two nearly degenerate and two soft triangles it agrees to the accuracy of the quadrature, which is 30 to 34 digits. The record of these comparisons is part of the ancillary files.

A.5 Limits

We note three limits of eq. (26) for later use. For an equilateral triangle with $X_v = X$ all three arguments are $u_i = \frac{1}{3}$, and

$$\int \mathrm{d}^3\ell\;\psi_3 \;=\; \frac{\pi}{3X^3}\Big[\,11\,\mathrm{Li}_2\big(\tfrac{1}{3}\big)+16\ln^2\tfrac{2}{3}-\frac{2\pi^2}{3}\Big]\,. \tag{56}$$

When the momentum at site 1 becomes soft, the other two site energies approach a common value X. The result is finite and has no logarithm of X_1,

$$\int \mathrm{d}^3\ell\;\psi_3 \;\longrightarrow\; \frac{3\pi}{32\,X^3}\,, \qquad X_1\to 0\,. \tag{57}$$

For a degenerate triangle with $X_1 = X_2+X_3$ the denominator of eq. (26) vanishes to second order in ξ_1. The numerator vanishes to the same order by the identity $\mathrm{Li}_2(t)+\mathrm{Li}_2(1-t) = \frac{\pi^2}{6} - \ln t\,\ln(1-t)$. With $s = X_2+X_3$ and $t = X_3/s$ the limit is

$$\int \mathrm{d}^3\ell\;\psi_3 \;\longrightarrow\; \frac{\pi}{96\,s^3\,t^2(1-t)^2}\,N(t)\,, \qquad \xi_1\to 0\,, \tag{58}$$

$$\begin{aligned} N(t) \;=\;& 6\,(2t^3-3t^2+3t-1)\,\mathrm{Li}_2(t)+6\,t\,(t^2-t+1)\ln t\,\ln(1-t)-3\,t^2(t-2)\ln t \\ &+3\,(t^3-t^2-t+1)\ln(1-t)-\pi^2t^3-9\,t^2+9\,t\,. \end{aligned} \tag{59}$$

A.6 Relation to other bootstrap methods

Three approaches in cosmology carry the name bootstrap, and they use singularities in different ways. The non-perturbative de Sitter bootstrap [32] imposes unitarity and crossing as constraints on the space of theories. The cosmological bootstrap [1, 2] and its descendants at loop level [33–37] solve for correlators from symmetries and singularities. The approach used here fixes individual integrals in whatever function space their geometry requires, and tests the result against numerical values. The three are complementary. The present paper also illustrates a limitation of the third. The function space suggested by the cuts of the master integrals can be larger than the one that the physical quantity needs.

B Derivations for the box

In this appendix we derive the results of section 6. We first derive the residue at the pole of a single site and the geometry of the threshold. We then reduce D_0 to Carlson integrals. The remaining subsections concern the line of section 6.5. They give the periods of its elliptic curves, the conditions that fix u and v, and the expansion at large site energy, where the constant Ω appears.

B.1 The residue at the pole of a single site

The pole at $X_1 + y_{41} + y_{12} = 0$ comes from the region of the time integrals in which t_1 is larger than the times of the two neighbouring sites. For $t_1 > t_2$ the propagator (5) factorizes,

$$G_{y_{12}}(t_1, t_2) \;=\; \frac{e^{-y_{12}t_1}}{2y_{12}} \left(e^{\,y_{12}t_2} - e^{-y_{12}t_2}\right), \tag{60}$$

and the same holds for $G_{y_{41}}(t_1, t_4)$. The integral over t_1 from the larger of t_2 and t_4 to infinity is then

$$\int_{\max(t_2,t_4)}^{\infty} \mathrm{d}t_1\; e^{-(X_1+y_{41}+y_{12})\,t_1} \;=\; \frac{e^{-(X_1+y_{41}+y_{12})\max(t_2,t_4)}}{X_1 + y_{41} + y_{12}}\,. \tag{61}$$

On the pole the exponential on the right-hand side equals one, and the residue is an integral over the times of the other three sites. Each of the two brackets of the form (60) shifts the energy of a neighbouring site by $\pm y$, with a sign. The remaining integral is that of the chain of sites 2, 3 and 4, which gives eq. (36). We have checked eq. (36) against the recursion for ψ_4 in exact arithmetic.

B.2 The threshold

On the pole the sum of the distances from $\vec{\ell}$ to two fixed points is constant. The points are the foci at which y_{12} and y_{41} vanish, and they are a distance P_1 apart. The loop momentum therefore lies on a spheroid. At the threshold $y_{41} + y_{12} = P_1$ the spheroid collapses onto the segment between the foci, on which $y_{12} = \frac{1}{2}(P_1 - d)$ and $y_{41} = \frac{1}{2}(P_1 + d)$. The distance from a point of the segment to a third point follows from Stewart's theorem. Let C be a point at distance a from the focus at which y_{12} vanishes and at distance b from the other focus. The theorem gives

$$|\vec{\ell} - \vec{C}|^2 \;=\; \frac{(P_1 + d)\,a^2 + (P_1 - d)\,b^2}{2P_1} - \frac{P_1^2 - d^2}{4}\,. \tag{62}$$

With the two remaining vertices of the quadrilateral in place of C this is eq. (38). Both $q_{23} = y_{23}^2$ and $q_{34} = y_{34}^2$ are quadratic in d with leading coefficient $\frac{1}{4}$. We write

$$q_{23} \;=\; \tfrac{1}{4}\,(d - e_1)(d - e_2)\,, \qquad q_{34} \;=\; \tfrac{1}{4}\,(d - e_3)(d - e_4)\,, \qquad s^2 \;=\; \prod_{i=1}^{4}(d - e_i)\,, \tag{63}$$

so that $s^2 = 16\,q_{23}\,q_{34}$. The roots are

$$e_{1,2} \;=\; -m \pm \sqrt{m^2 - n}\,, \qquad m = \frac{P_2^2 - P_{12}^2}{P_1}\,, \qquad n = 2\big(P_2^2 + P_{12}^2\big) - P_1^2\,, \tag{64}$$

and $e_{3,4}$ follow with $P_2 \to P_{41}$ and $P_{12} \to P_4$. For momenta that do not lie in a plane the roots form two complex-conjugate pairs.

B.3 Reduction of D_0 to Carlson integrals

The integrand of eq. (39) is a rational function of d, y_{23} and y_{34}. We separate it according to its parity under $y_{23} \to -y_{23}$ and $y_{34} \to -y_{34}$. The part that is even in both roots is rational in d. The parts that are odd in one root contain a single square root of a quadratic polynomial, and they integrate to logarithms. The part that is odd in both roots is a rational function of d divided by s, and it gives the elliptic integrals.

Each of the six linear factors in the denominator of eq. (37) vanishes at points $d = \alpha$ on one of the four sheets of the two roots. We label the sheets by the values $\eta = \pm y_{23}(\alpha)$ and $\eta' = \pm y_{34}(\alpha)$ of the roots at the pole. For momenta that do not lie in a plane all these poles are simple. Let ρ be the residue of the integrand at such a pole. The partial-fraction decomposition then gives

$$D_0 \;=\; \frac{\pi}{4P_1}\left[\,\frac{1}{4}\sum_{(\alpha,\eta,\eta')} \rho\,\Big(L_0 + \eta\, L_{23} + \eta' L_{34} + \eta\,\eta'\, L_\Pi\Big) + 4\, p_0\, J_F\right], \tag{65}$$

where the four functions of α are the integrals of the four parities,

$$L_0 = \int_{-P_1}^{P_1} \frac{\mathrm{d}d}{d-\alpha}\,, \qquad L_{23} = \int_{-P_1}^{P_1} \frac{\mathrm{d}d}{(d-\alpha)\, y_{23}}\,, \qquad L_\Pi = \int_{-P_1}^{P_1} \frac{\mathrm{d}d}{(d-\alpha)\, y_{23}\, y_{34}}\,, \tag{66}$$

and L_{34} is defined as L_{23} with y_{34} in place of y_{23}. The part that is odd in both roots has in addition a constant polynomial part, which multiplies the integral of the first kind $J_F = \int \mathrm{d}d/s$. Its coefficient follows from the partial fractions at the branch point $d = e_1$,

$$p_0 \;=\; \frac{1}{4}\sum_{(\alpha,\eta,\eta')} \frac{\rho\,\eta\,\eta'}{\alpha - e_1}\,. \tag{67}$$

The first two integrals in eq. (66) are elementary,

$$\begin{aligned} L_0 &= \log\frac{P_1-\alpha}{-P_1-\alpha}\,,\\ L_{23} &= -\frac{1}{\sqrt{q_{23}(\alpha)}}\left[\log\frac{2\, q_{23}(\alpha) + q_{23}'(\alpha)\,(d-\alpha) + 2\sqrt{q_{23}(\alpha)\, q_{23}(d)}}{d-\alpha}\right]_{d=-P_1}^{d=P_1}. \end{aligned} \tag{68}$$

For the elliptic integrals we use the symmetric integrals of Carlson [38]. With $r_i = \sqrt{P_1 - e_i}$ and $\bar r_i = \sqrt{-P_1 - e_i}$ we define

$$U_{ij} \;=\; \frac{r_i\, r_j\, \bar r_k\, \bar r_l + \bar r_i\, \bar r_j\, r_k\, r_l}{2P_1}\,, \tag{69}$$

where i, j, k and l are distinct. The integral of the first kind is

$$J_F \;=\; \int_{-P_1}^{P_1} \frac{\mathrm{d}d}{s} \;=\; 2\, R_F\big(U_{12}^2, U_{13}^2, U_{14}^2\big)\,. \tag{70}$$

Since $s = 4\, y_{23}\, y_{34}$, the integral of the third kind is $L_\Pi = 4\,(J_\Pi - J_F)/(\alpha - e_1)$ with

$$J_\Pi \;=\; \int_{-P_1}^{P_1} \frac{(d-e_1)\,\mathrm{d}d}{(d-\alpha)\, s} \;=\; \frac{2\, d_{12}\, d_{13}\, d_{14}}{3\, d_{15}}\; R_J\big(U_{12}^2, U_{13}^2, U_{14}^2, U_{15}^2\big) + \frac{1}{w}\,\log\frac{S_5 + w}{S_5 - w}\,, \tag{71}$$

where $d_{ij} = e_j - e_i$ with $e_5 = \alpha$, and

$$\begin{aligned} U_{15}^2 &= U_{12}^2 - \frac{d_{13}\, d_{14}\, d_{25}}{d_{15}}\,, \qquad w^2 = S_5^2 + \frac{(P_1^2 - \alpha^2)\, U_{15}^2}{r_1^2\, \bar r_1^2}\,,\\ S_5 &= \frac{1}{2P_1}\left[\frac{r_2\, r_3\, r_4}{r_1}\,(-P_1 - \alpha) + \frac{\bar r_2\, \bar r_3\, \bar r_4}{\bar r_1}\,(P_1 - \alpha)\right]. \end{aligned} \tag{72}$$

Equations (65) to (72) are the complete result. The branches of the logarithm and of the Carlson integrals must be chosen by continuation from $d = -P_1$. The formulas in terms of R_F and R_J hold on an interval on which the real quantities U_{ij} are positive. If one of them changes sign on the segment, the segment is divided at that point, and the integrals of the pieces are added. Poles at the end points $\alpha = \pm P_1$ contribute their finite parts, and real poles inside the interval contribute principal values. The ancillary files contain an evaluator that implements these rules. For momenta in a plane the factor $P_3 + y_{23} + y_{34}$ has a double zero on one sheet. The decomposition (65) then needs an additional term, which we have not derived.

The monodromy of D_0 quoted in section 6.3 was obtained by numerical continuation in one of the lengths of the quadrilateral. For two quadrilaterals that do not lie in a plane it contains elements with integer traces 4, 6, 18 and 20. In the exact test the module generated by the residue (36) has rank six on one family of quadrilaterals and rank four on a second family. In both cases it contains the module of rank two of the periods of the curve, whereas a logarithmic form on the same curve generates a module of rank one.

B.4 The elliptic curves on the line

On the line of section 6.5 three elliptic curves appear. They are the curves on which the energies of two subgraphs vanish. The two subgraphs are two adjacent sites, two opposite sites, or one site and the pair of adjacent sites that contains it. We denote the curves by $E_{\rm adj}$, $E_{\rm opp}$ and $E_{\rm nest}$.

The periods of all three are hypergeometric functions of the j-invariant. To see this, we bring a curve to the form $y^2 = 4x^3 - g_2\,x - g_3$. Its periods are homogeneous under the rescaling $g_2 \to \lambda^4 g_2$ and $g_3 \to \lambda^6 g_3$, which multiplies them by λ^{-1}. A period is therefore $g_2^{-1/4}$ times a function of the invariant ratio

$$J \;=\; \frac{1728}{j} \;=\; 1 - \frac{27\,g_3^2}{g_2^3}\,. \tag{73}$$

This function obeys the hypergeometric equation with parameters $\frac{1}{12}$, $\frac{5}{12}$ and 1. For $0 < J < 1$ and $g_3 > 0$ the real period is

$$\omega \;=\; \frac{2\pi}{(12\,g_2)^{1/4}}\; {}_2F_1\big(\tfrac{1}{12}, \tfrac{5}{12}; 1; J\big)\,. \tag{74}$$

For $g_3 < 0$ the same expression is the modulus of the imaginary period. In both cases it is the period of smallest modulus. On the line j is a rational function of degree 24 in t for each curve. We denote by c_4 the polynomial of degree eight whose cube is the numerator of j, which is proportional to g_2 in a suitable model of the curve. The second-order operator $\mathcal{L}_E$ of each curve is therefore the hypergeometric operator in the variable $J(t)$, conjugated by $c_4^{1/4}$,

$$\mathcal{L}_E \;=\; c_4^{-1/4}\left[\,J(1-J)\,\frac{\mathrm{d}^2}{\mathrm{d}J^2} + \Big(1 - \frac{3J}{2}\Big)\frac{\mathrm{d}}{\mathrm{d}J} - \frac{5}{144}\,\right] c_4^{1/4}\,, \tag{75}$$

with both sides normalized to unit leading coefficient in $\mathrm{d}/\mathrm{d}t$. We have verified eq. (75) exactly for the three operators obtained from the reduction. The point $J = 0$ is $j = \infty$, where a curve degenerates. This happens at $t \to 0$ for all three curves and at the threshold $t = -1 + \sqrt{3/2}$ of $E_{\rm opp}$. In none of the three cases is t a modular function for the curve. Each map $t \mapsto j$ has critical points away from $j = 0$, 1728 and ∞, which are the apparent singularities of $\mathcal{L}_E$. We give the three j-invariants in the ancillary files.

B.5 The fifth-order operator

The operator of order five of section 6.4 arises in three ways. It is the operator of the periods of the surface as a function of $\sigma = y_{41} + y_{12}$. It is the operator of the same surfaces along the line $X_v = 1 + t$, on which the pole of site 1 lies at $\sigma = -(1 + t)$. It is also the block of order five of the reduction on that line. With the substitution $\sigma \to 1 + t$ the three operators are identical. The symmetric square of the operator has order 14 and not 15. The missing solution is the quadratic relation among the five periods. The solutions are free of logarithms at infinite σ.

The coupling of the physical integrand to this block can be tested on the function. For momenta that form a regular tetrahedron of unit side the solutions of the block have branch points at the roots σ_c of $\sigma^4 - 4\sigma^2 + 12$. A function that contains the block inherits a term proportional to $(\sigma - \sigma_c)^{5/2}$. Its coefficient is fixed by the residue (36) at the point where two singular points of the surface collide. The single-site discontinuity at one leg per site has this branch point, with an exponent of 2.507 and with the predicted coefficient. With several legs per site the leading term of the residue at large site energies generates the full block in exact arithmetic, whereas a form of the opposite parity generates none of it. In the exact test at one leg per site the module generated by the integrand of the coefficient has dimension 36, and that of the correlator has dimension 34. The quotient of the former by the remaining forms on the single-site pole has dimension five, and its operator is the operator of order five.

B.6 The physical solutions on the line

The reduction on the line gives first-order systems for the master integrals and their coefficients in the expansion in ε. The master integrals have double poles in ε. The systems that account for them have dimension 81 for the coefficient and 67 for the correlator. The coefficient of the double pole of each master integral is a residue at infinite loop momentum, and it equals 0, $-\pi/8$ or $-\pi/16$. With these values the physical functions lie in quotient systems of dimension 34 for the coefficient and 28 for the correlator. Each elliptic block occurs twice, once for each order of the pole in ε. Only the copies attached to the simple pole contribute to the physical functions.

The loop integral converges for $t > -1$, so that the physical solution is single-valued around the singular points of the system in that range. In the system of dimension 28 the solutions that are single-valued around the six points

$$t \;=\; 1\,, \quad -1+\sqrt{\tfrac{3}{2}}\,, \quad 0\,, \quad -1+\tfrac{1}{\sqrt{2}}\,, \quad -1+\tfrac{2}{\sqrt{13}}\,, \quad -\tfrac{1}{2} \tag{76}$$

form a space of dimension four. Those that are also single-valued around the logarithmic point $t = -\frac{2}{3}$ form a space of dimension three. For the coefficient the corresponding dimensions are eight and seven. We have not imposed the condition at the remaining point $t = -1+1/\sqrt{10}$. Exactly one solution in these spaces is free of logarithms at large X. This is the function v, which we normalize to begin with X^{-4}. Its expansion is even in $1/X$ and has rational coefficients,

$$v \;=\; X^{-4} + \frac{29}{80}\,X^{-6} + \frac{923}{12800}\,X^{-8} - \frac{1531}{204800}\,X^{-10} + O\big(X^{-12}\big)\,. \tag{77}$$

The function u is the solution with $\alpha_4 = 0$ that has the exact coefficients β_4 to β_8 and α_5 of the next subsection, and whose three boundary constants attached to the double poles equal $-\pi/8$. None of these conditions constrains the coefficient of v, and the condition at $t = -\frac{2}{3}$ does not constrain it either.

B.7 The expansion at large site energy

We now derive the leading coefficients of eq. (43). At large X the loop integral receives contributions from two regions, which we separate in $d = 3-2\varepsilon$ dimensions. In the soft region the loop momentum is of order one. The integrand of the correlator is then expanded in y_e/X, and the term of order X^{-4-m} is a polynomial of degree m in the edge energies divided by their product. In the hard region the loop momentum is of order X. The integrand is homogeneous of degree -8, so that this region starts at order $X^{-5-2\varepsilon}$. Poles in ε cancel between the two regions and leave logarithms of X.

The leading term comes from the soft region alone, and it is $\Omega\, X^{-4}$ with Ω defined in eq. (42). To reduce Ω we introduce one Feynman parameter x_e for each factor $1/y_e = 1/|\vec{\ell} - \vec{A}_e|$, where the $\vec{A}_e$ are the vertices of the regular tetrahedron. The denominator becomes

$$\sum_e x_e\,(\vec{\ell} - \vec{A}_e)^2 \;=\; \Big(\vec{\ell} - \sum_e x_e \vec{A}_e\Big)^2 + \sum_{e<f} x_e\, x_f \tag{78}$$

on the simplex $\sum_e x_e = 1$, because all distances between the vertices equal one. The Feynman-parameter formula for four factors of power one half has the prefactor $1/\pi^2$. With $\int \mathrm{d}^3\ell\,(\ell^2+\Delta)^{-2} = \pi^2\,\Delta^{-1/2}$ the loop integral can be done, and

$$\Omega \;=\; \int_{\sum x=1} \frac{\mathrm{d}^3x}{\sqrt{x_1x_2x_3x_4}\,\sqrt{e_2(x)}}\,, \qquad e_2(x) = \sum_{e<f} x_e\, x_f\,. \tag{79}$$

One further integration gives a two-dimensional integral over elementary functions,

$$\Omega \;=\; 8\int_0^{\pi/2}\!\!\int_0^{\pi/2} \mathrm{d}\phi_1\,\mathrm{d}\phi_2\, \frac{1}{\sqrt{1-\frac{1}{4}(s_1+s_2)}}\, \arcsin\frac{1-\frac{1}{2}s_1}{\sqrt{1-\frac{1}{4}s_1s_2}}\,, \qquad s_i = \sin^2 2\phi_i\,. \tag{80}$$

We have not been able to reduce it further.

At order X^{-5} the soft region contributes $-6\,T_3$, where T_3 is the same integral with three of the four factors. The steps that led to eq. (79) now give

$$T_3 \;=\; \int \mathrm{d}^d\ell\, \frac{1}{y_1\,y_2\,y_3} \;=\; \pi^{-\varepsilon}\,\Gamma(\varepsilon) \int_{\sum x=1} \frac{\mathrm{d}^2x}{\sqrt{x_1x_2x_3}}\, e_2(x)^{-\varepsilon} \;=\; \frac{2\pi}{\varepsilon} - 2\pi\big(\gamma_E + \log\pi\big) - J_1 + O(\varepsilon)\,, \tag{81}$$

with

$$\int_{\sum x=1} \frac{\mathrm{d}^2x}{\sqrt{x_1x_2x_3}} = 2\pi\,, \qquad J_1 = \int_{\sum x=1} \frac{\mathrm{d}^2x}{\sqrt{x_1x_2x_3}}\, \log e_2(x) = 4\pi\log 3 - 8\pi\,. \tag{82}$$

The pole of the soft region is therefore $-12\pi/\varepsilon$. The hard region has the opposite pole, multiplied by $X^{-2\varepsilon}$. The sum is finite and contains the logarithm $-24\pi\, X^{-5}\log X$, which is the coefficient β_5 of eq. (43). The finite parts combine to

$$\alpha_5 \;=\; \frac{\pi}{12}\big(22 + 291\log 3 - 108\log 2\big)\,. \tag{83}$$

The higher orders follow in the same way. Each soft term is a one-loop integral with simple poles only, so that no higher power of the logarithm appears. A logarithm requires an ultraviolet pole of a soft term, which exists only at odd orders, so that $\beta_n = 0$ for even n. We find

$$\alpha_6 = -\frac{95}{3}\,\pi + 8\,\widetilde{\Omega}\,, \qquad \beta_7 = -\frac{158}{3}\,\pi\,, \qquad \alpha_7 = \pi\Big(\frac{22519}{360} + \frac{423}{8}\log 3 - 16\log 2\Big)\,, \tag{84}$$

where $\widetilde{\Omega} = -3.3142572208468856411918120617$ is the dimensionally regularized value of the integral in eq. (42) with y_{12}^{-1} replaced by y_{12}. In terms of eq. (77) the coefficients are $\alpha_n = a_n\,\Omega + u_n$, where a_n are the coefficients of v, and all logarithms belong to u. The next two logarithms are $\beta_9 = -\frac{627}{10}\pi$ and $\beta_{11} = \frac{10247}{840}\pi$, which the numerical values confirm to 12 and 8 digits. The series converges for $|X| > 2$, beyond the outermost singular point of the system. The numbers Ω and $\widetilde{\Omega}$ are known numerically only.

B.8 The coefficient

For the coefficient V_4 the integrand has no factor $1/\prod_e y_e$, and the expansion at large X starts at X^{-5}. Its coefficients through X^{-11} are known exactly as rational combinations of π, $\pi\log 2$ and $\pi\log 3$. The first logarithm appears at X^{-11} with $\beta_{11} = -\frac{11}{21}\pi$. On the space of dimension eight these conditions leave two directions that are free of logarithms at large X, both of which enter at X^{-12}. At present $V_4 = u_\psi + \Omega_1' v_1 + \Omega_2' v_2$ with two undetermined constants. Single-valuedness at $t = -1 + 1/\sqrt{10}$ imposes one further condition and is expected to remove one of them. We expect the remaining constant to be the analogue of Ω in which the product of the four edge energies replaces its inverse. We have not shown this.

References

[1] N. Arkani-Hamed, D. Baumann, H. Lee and G.L. Pimentel, *The Cosmological Bootstrap: Inflationary Correlators from Symmetries and Singularities*, *JHEP* **04** (2020) 105 [1811.00024].

[2] D. Baumann, D. Green, A. Joyce, E. Pajer, G.L. Pimentel, C. Sleight et al., *Snowmass White Paper: The Cosmological Bootstrap*, 2203.08121.

[3] N. Arkani-Hamed, P. Benincasa and A. Postnikov, *Cosmological Polytopes and the Wavefunction of the Universe*, 1709.02813.

[4] N. Arkani-Hamed, D. Baumann, A. Hillman, A. Joyce, H. Lee and G.L. Pimentel, *Kinematic Flow and the Emergence of Time*, *Phys. Rev. Lett.* **135** (2025) 031602 [2312.05300].

[5] N. Arkani-Hamed, D. Baumann, A. Hillman, A. Joyce, H. Lee and G.L. Pimentel, *Differential equations for cosmological correlators*, *JHEP* **09** (2025) 009 [2312.05303].

[6] S. De and A. Pokraka, *Cosmology meets cohomology*, *JHEP* **03** (2024) 156 [2308.03753].

[7] A. Hillman, *Symbol Recursion for the dS Wave Function*, 1912.09450.

[8] S. He, X. Jiang, J. Liu, Q. Yang and Y.-Q. Zhang, *Differential equations and recursive solutions for cosmological amplitudes*, *JHEP* **01** (2025) 001 [2407.17715].

[9] P. Benincasa, G. Brunello, M.K. Mandal, P. Mastrolia and F. Vazão, *One-loop corrections to the Bunch-Davies wave function of the universe*, *Phys. Rev. D* **111** (2025) 085016 [2408.16386].

[10] Y. Hang and C. Shen, *A note on kinematic flow and differential equations for two-site one-loop graph in FRW spacetime*, *JHEP* **09** (2025) 209 [2410.17192].

[11] D. Baumann, H. Goodhew and H. Lee, *Kinematic flow for cosmological loop integrands*, *JHEP* **07** (2025) 131 [2410.17994].

[12] S. Laporta and E. Remiddi, *Analytic treatment of the two loop equal mass sunrise graph*, *Nucl. Phys. B* **704** (2005) 349 [hep-ph/0406160].

[13] S. Bloch and P. Vanhove, *The elliptic dilogarithm for the sunset graph*, *J. Number Theor.* **148** (2015) 328 [1309.5865].

[14] L. Adams, C. Bogner and S. Weinzierl, *The two-loop sunrise graph with arbitrary masses*, *J. Math. Phys.* **54** (2013) 052303 [1302.7004].

[15] T. Heckelbacher, I. Sachs, E. Skvortsov and P. Vanhove, *Analytical evaluation of cosmological correlation functions*, *JHEP* **08** (2022) 139 [2204.07217].

[16] G.L. Pimentel and T. Westerdijk, *On Cosmological Correlators at One Loop*, 2601.00952.

[17] J. Henn, J. Mei and Q. Yang, *A compact analytic formula for the one-loop triangle cosmological correlator*, 2608.17877.

[18] S. Agui Salcedo and S. Melville, *The cosmological tree theorem*, *JHEP* **12** (2023) 076 [2308.00680].

[19] C. Chowdhury, A. Lipstein, J. Mei, I. Sachs and P. Vanhove, *The Subtle Simplicity of Cosmological Correlators*, 2312.13803.

[20] K. Acres and D. Broadhurst, *Empirical determinations of Feynman integrals using integer relation algorithms*, 2103.06345.

[21] J. Broedel, C. Duhr, F. Dulat and L. Tancredi, *Elliptic polylogarithms and iterated integrals on elliptic curves. Part I: general formalism*, *JHEP* **05** (2018) 093 [1712.07089].

[22] L. Adams and S. Weinzierl, *The ε-form of the differential equations for Feynman integrals in the elliptic case*, *Phys. Lett. B* **781** (2018) 270 [1802.05020].

[23] J.L. Bourjaily et al., *Functions Beyond Multiple Polylogarithms for Precision Collider Physics*, in *Snowmass 2021*, 3, 2022 [2203.07088].

[24] S. Agui Salcedo, M.H.G. Lee, S. Melville and E. Pajer, *The Analytic Wavefunction*, *JHEP* **06** (2023) 020 [2212.08009].

[25] A.B. Goncharov, M. Spradlin, C. Vergu and A. Volovich, *Classical Polylogarithms for Amplitudes and Wilson Loops*, *Phys. Rev. Lett.* **105** (2010) 151605 [1006.5703].

[26] C. Chowdhury, A. Lipstein, J. Marshall, J. Mei and I. Sachs, *Cosmological dressing rules*, *JHEP* **03** (2026) 076 [2503.10598].

[27] C. Chowdhury, S. Jazayeri, A. Lipstein, J. Marshall, J. Mei and I. Sachs, *Cosmological Correlator Discontinuities from Scattering Amplitudes*, 2602.03841.

[28] C. Chowdhury, S. He, Y.-X. Su and D. Yang, *On the simplicity of de Sitter correlators*, *JHEP* **08** (2026) 205 [2604.26421].

[29] A. Bzowski, P. McFadden and K. Skenderis, *Implications of conformal invariance in momentum space*, *JHEP* **03** (2014) 111 [1304.7760].

[30] Z. Qin and Z.-Z. Xianyu, *Cosmological Collider Signals From a Triangle Loop*, 2609.09288.

[31] M. Borinsky, A. Herderschee and Q. Lu, *On the Numerical Integration of One-Loop Cosmological Collider Signals*, 2609.10673.

[32] M. Hogervorst, J. Penedones and K. Salehi Vaziri, *Towards the non-perturbative cosmological bootstrap*, 2107.13871.

[33] Z.-Z. Xianyu and H. Zhang, *Bootstrapping One-Loop Inflation Correlators with the Spectral Decomposition*, *JHEP* **04** (2023) 103 [2211.03810].

[34] H. Liu, Z. Qin and Z.-Z. Xianyu, *Dispersive Bootstrap of Massive Inflation Correlators*, 2407.12299.

[35] H. Liu, Z. Qin, J. Wu, Z.-Z. Xianyu and H. Zhang, *On-Shell Bootstrap of Loop Inflation Correlators with Spectral Dispersion*, 2606.02686.

[36] T. Westerdijk and C. Yang, *Bananas are Unparticles: Differential Equations and Cosmological Bootstrap*, *JHEP* **09** (2025) 089 [2503.08775].

[37] S. Paranjape, M. Skowronek, M. Spradlin, A. Volovich and H.-C. Weng, *Cluster Bootstrap for Cosmological Correlators*, 2603.08670.

[38] B.C. Carlson, *Numerical computation of real or complex elliptic integrals*, *Numer. Algorithms* **10** (1995) 13 [math/9409227].